

BRINE TRANSPORT IN SEDIMENTARY BASINS OVER GEOLOGICAL TIMESCALES

MASTER THESIS

M.SC. HYDROGEOLOGY AND ENVIRONMENTAL GEOSCIENCE

By Mohamed Benhsinat

Matriculation Number: 21364982

Supervisors

1. Dr. Elco Luijendijk
2. Dr. Hanneke Verweij

Accomplished at the
Department of Structural Geology and Geodynamics
Faculty of Geosciences and Geography
Georg-August Universität
Göttingen

Supervisor

Dr. Elco Lujendijk
Department of Structural Geology and Geodynamics ...
Faculty of geosciences and geography
Goldschmidtstraße 3, 37077 Göttingen

Co-supervisor

Dr. Hanneke Verweij.....
TNO Geological survey of the Netherlands.....
Princetonlaan 6, 3584 CB Utrecht
The Netherlands

DECLARATION

I hereby certify that this thesis has been composed by me and is based on my own work, unless stated otherwise. No other person's work has been used without due acknowledgement in this thesis. All references and verbatim extracts have been quoted, and all sources of information, including graphs and data sets, have been specifically acknowledged.

.....
Date, Signature

ACKNOWLEDGEMENTS

First, I would like to express my gratitude to my master thesis supervisor Dr. Elco Luijendijk for his guidance throughout the period of this research, his constructive criticism and friendly advice. I would like to acknowledge him for his expertise in numerical modelling.

His continuous suggestions are the main reasons to complete this work. He has offered his time whenever I needed. He was continuously reviewing my results and has helped me to finalize this report.

I would also like to thank Dr. Hanneke Verweij as my co-supervisor for the data provided.

Last but not least, I would like to thank my family (parents and brothers) for supporting me throughout my life.

TABLE OF CONTENTS

DECLARATION	iii
ACKNOWLEDGEMENTS	iv
TABLE OF CONTENTS	v
LIST OF FIGURES	vii
LIST OF TABLES	viii
Abstract	ix
I. Introduction	1
II. Background and description	3
1. Study area	3
a. Geological history and stratigraphy	3
b. Netherlands coast line evolution and deposits during Tertiary and Quaternary	5
• Mid Paleocene to earliest Eocene deposits	5
• Oligocene deposits	6
• Miocene to middle Quaternary deposits	7
• Pleistocene/Holocene deposits and sea level evolution	8
c. Netherlands Zechstein group	10
d. Wells	12
2. Solute diffusion	13
III. Methods and materials	15
1. Resistivity to pore water salinity	15
2. Single well diffusion model.....	16
a. Model code.....	16
b. Input well	21
3. Modelling diffusion for multiple synthetic wells	22
IV. Results and discussion	24
1. Resistivity to pore water salinity	24
a. Results and discussion	24
2. Diffusion model	27
a. Single well diffusion	27
i. Results	27
ii. Discussion	28

b. Multiple synthetic wells diffusion.....	29
i. Results.....	29
ii. Discussion.....	33
Conclusion.....	37
References.....	38
Appendix.....	40

LIST OF FIGURES

Figure 1: Netherlands’s basin chronostratigraphy	4
Figure 2: Type of deposits from Mid Paleocene to earliest Eocene – modified	5
Figure 3: Type of deposits from Mid-Eocene to Late Oligocene-modified.....	6
Figure 4: Type of deposits from Miocene to middle Quaternary –Modified.....	7
Figure 5: Quaternary chronology and the associated mean July temperatures	8
Figure 6: Coastline extension during Pleistocene/Holocene.....	9
Figure 7: Surface deposits of the Netherlands	10
Figure 8: Zechstein layers	11
Figure 9: The location of wells AST, NDW used to construct input files	12
Figure 10: Model-code run-time	18
Figure 11: Model domain.....	20
Figure 12: Synthetic salinity wells created from digital geological maps of the Netherlands	23
Figure 13: The thickness of synthetic wells at every group of strata.....	24
Figure 14: Comparison of calculated salinity using resistivity log data with observed salinity data in well AST-02.....	25
Figure 15: Comparison of resistivity log ILD with measured Salinity for well AST-02.....	26
Figure 16: Result of the diffusion model for a fixed and variable diffusion coefficient.....	27
Figure 17: Results of Pybasin model: Burial history and salinity output for borehole AST-02	28
Figure 18: Modeled Fresh-saline water interface (1g/l) using diffusion model for multiple synthetic wells	29
Figure 19: Fresh-Saline water interface (1g/L) modified	30
Figure 20: Difference between observed Fresh-saline water interface originated from (Stuurman et al., 2006) and diffusion only modeled fresh-saline interface (1g/L)	31
Figure 21: Depth in meter below NAP to the Zechstein modified	32
Figure 22: a-Distance to base of the Holocene (below NAP); b-surface geology of Netherlands; c- distance to base of Pleistocene (Below NAP).....	33
Figure 23: Hydrogeological cross section.....	34
Figure 24: Digital elevation model modified.....	36
Figure 25: Diffusion coefficient in water for some ions at 25 °C	40
Figure 26: Preview of Arcpy script for creating synthetic wells used in salinity diffusion model applied to Netherlands	40

LIST OF TABLES

Table 1: Location and Total vertical depth of the Wells AST-01, AST-02 and NDW-01	12
Table 2: Preview of the stratigraphy information file used as input for Pybasin model.....	17
Table 3: Well stratigraphy file for TestWell 1 used as input for Pybasin model.....	17
Table 4 : Stratification of input well AST-02 after extension.....	22
Table 5: Comparison between calculated salinities (for different cementation factor) and the measured one by TNO.....	25
Table 6: The stratification of Well NDW-01	42
Table 7 : Comparaision between ILD log and the measured salinity (log scale).....	43
Table 8: The stratification of Well AST-01	44

Abstract

Pore water salinity datasets may offer unique opportunity to trace fluid flow on geological timescales. This idea was used in the present research in order to explore to which extent, the salinity distribution can only be explained by diffusion of salts from evaporites. To proceed, a one dimension salinity diffusion model was built and added to an already developed Pybasin code (Luijendijk et al., 2011). Several synthetic wells based on geological maps (NL Oil and Gas Portal, 2015a) were used as model inputs. The predicted salinity results were first compared with the observed one of well AST-02 (Heederik et al., 1988) and after with a fresh-saline water interface map by Stuurman et al. (2006). It has been concluded that salinity distribution can not only be explained by diffusion process in the Netherlands, due to the existence of groundwater flow of higher magnitude in one hand. On the other hand, diffusion process even small, can have a strong effect whenever on long timescales.

I. Introduction

The knowledge of groundwater flow is important for quantifying water availability for agriculture, human consumption, ecosystems and can help to delineate contamination extent, and potential flooding areas. In some cases it might be also good to know how the groundwater was flowing in the past in order to plan for the future.

Information on how groundwater was flowing in the past is important for the storage of nuclear waste for example. These operations can only be done if the safety during the next million years is guaranteed. For that it's mandatory to learn from the past in order to predict somehow for the future. The question that arises then is how to know the behavior of groundwater in the past; in other words how the groundwater flow evolves over geological timescales. Neither isotope dating, nor available present data will be for a good help because timescale is millions of years. However pore water salinity data can provide valuable information on the chemical, hydrological, thermal and tectonic evolution of the crust's earth (Hanor, 1994). It offers an opportunity to trace fluid flow on geological timescales.

Topography driven flow has tendency to flush saline pore water from the up subsurface, whereas diffusion from evaporites tend to increase the pore water salinity. Since water is moving in porous material, salt got stuck and can remain in pores, so the distribution of salt can provide hints about the fluid flow in the past. Hence the distribution of Salinity can be used as a tracer of water flow. Numerous salinity dataset can provide a high resolution image of water flow.

The aim of this work is to use salinity dataset to build an image of groundwater flow over geological times. It will be more focused on diffusion process rather than topography gradient process and applied in Netherlands due to the available groundwater salinity data. The work is mainly on sedimentary basins because sediments keep thermal, salt records for a long time, the thing that is required in this present study.

As a first step, I tested a method to convert resistivity to salinity that used available log-resistivity data from the Netherlands Oil and Gas Portal. In addition I used detailed salinity data from boreholes. The salinity data were compared with predicted salinity from a simple modified 1D diffusion model PyBasin. This model was originally built by (Luijendijk et al.,

2011) and modified to include solute diffusion process. Finally I used the model to simulate salinity in 10573 synthetic wells, that were created on a 2 x 2 km grid of the Netherlands using Arcpy scripting and available digital geological models of the subsurface of the Netherlands (van Adrichem Boogaert and Kouwe, 1993), (Heederik et al., 1988). The results were interpolated to map the depth of the predicted fresh-salt water transition. Comparison with existing maps of the salt-freshwater transition (Stuurman et al., 2006) provides information about the effect of groundwater flow on pore water salinity.

II. Background and description

1. Study area

Netherlands was the study area because of data availability, some data were provided by the geological survey of the Netherlands and others are open access on the web. In addition this country was covered so many times by the sea, so it is the best place for testing pore water salinity to trace fluid flow on geological timescales.

a. Geological history and stratigraphy

Netherlands is situated in the North Sea sedimentary basin, a large part of the country is below sea level and have been several times flooded in the past (de Vries, 2007). Elevation ranges from below sea level to a maximum elevation of 320 meter above NAP (NAP = approximately mean sea level). Other relatively high areas located in the central eastern part are the ice pushed hills (107 meter above sea level) (de Vries, 2007).

The geological history of Netherlands is made up of three parts, the Paleozoic, the Mesozoic and the Cenozoic (*figure 1*). Every part has its specific interest in the present work.

- The geology of the first several hundred meters (Cenozoic) consists of formation deposited in the Tertiary and quaternary (Dufour, 1998). The quaternary is divided into two epochs: the Pleistocene and the Holocene (Dufour, 1998). These formations participate in the present day hydrological cycle (de Vries, 2007)
- The Mesozoic, especially the Cretaceous deposits in Limburg and Overijssel provinces, have older fresh groundwater in their interstitial pores at relatively shallower depth (Dufour, 1998).
- Paleozoic is a broadly regressive Carboniferous sequence. The layer on top of this layer is about 250 million years old (the Permian era). During this era, a large quantity of rock salt were produced (Zechstein) (de Jager, 2007).

The chronostratigraphy of the Netherlands is shown in figure below:

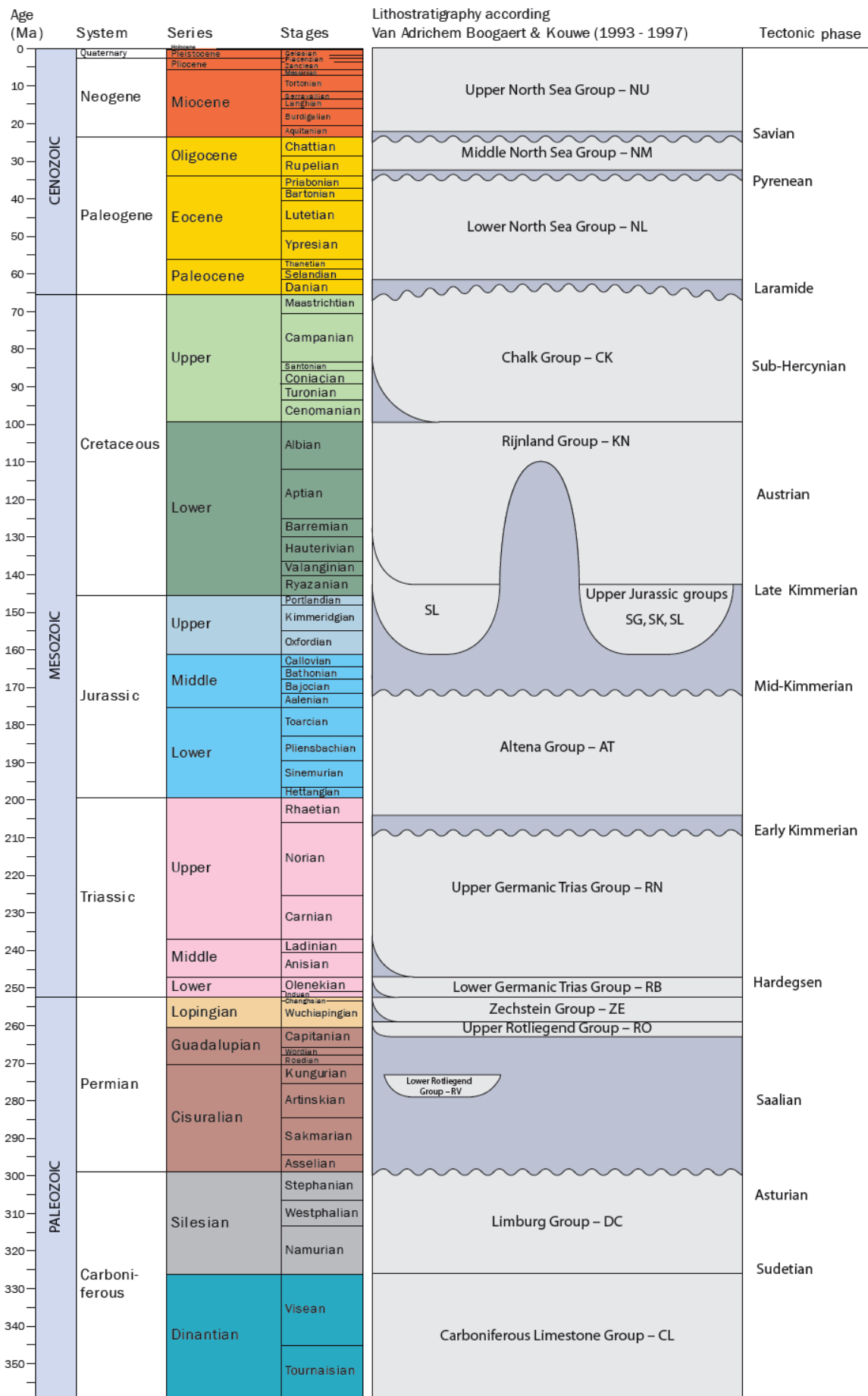


Figure 1: Netherlands's basin chronostratigraphy

Geological time scale (after Gradstein et al, 2004) and lithostratigraphic column (after Van Adrichem Boogaert & Kouwe, 1993 - 1997) showing main tectonic deformation phases.

Source: <https://www.dinoloket.nl/table>

b. Netherlands coast line evolution and deposits during Tertiary and Quaternary

Sea has invaded Netherlands many times during the past due to sea level increase and tectonic events (subsidence for example)(Zagwijn, 1989). Therefore deposits have changed during different periods between marine, terrestrial and brackish (*figures below*)

- Mid Paleocene to earliest Eocene deposits

According to Schnetler (2001) and Clemmensen & Thomsen (2005) sea-level has raised in the early Thanetian leading to a marine sedimentation extending to Netherlands, south east – England, Belgium and much of Germany. This sedimentation phase ended in Latest Ypresian times by a major influx of sand in the southern basin marginal area (*figure 2-d*)

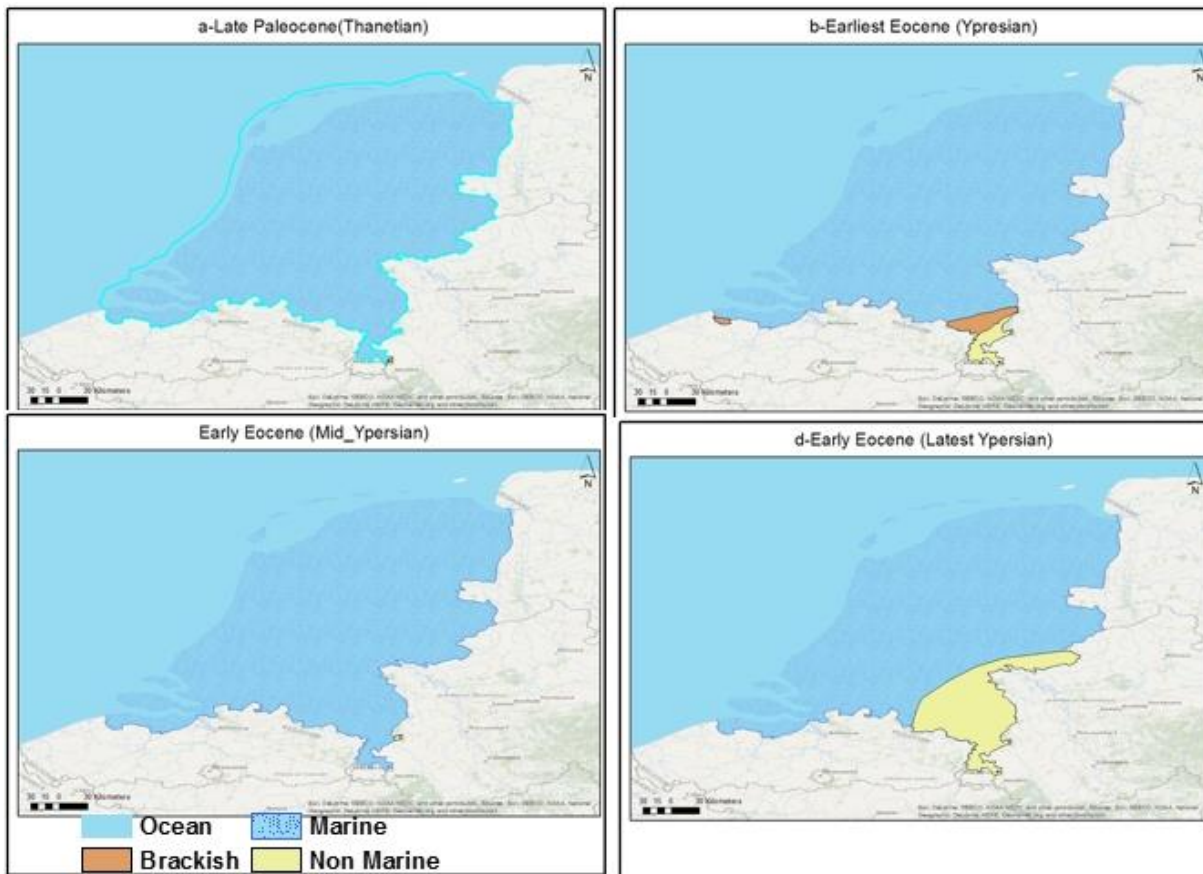


Figure 2: Type of deposits from Mid Paleocene to earliest Eocene – modified

- a. Late Paleocene (Thanetian: 58 Ma); b. Earliest Eocene (Ypresian: 56.5 Ma); c. Early Eocene (mid-Ypresian: 52.5 Ma);
 d. Early Eocene (latest Ypresian: 49 Ma).

Source: Based on the regional maps of Vinken (1988), Ziegler (1990), Ahmadi et al. (2003) and Jones et al. (2003), together with maps of Lotsch (1969, 2002), Thiry & Dupuis (1998), Martiklos (2002), Piwocki (2004), Gürs (2005), Heilmann-Clausen (2006), King (2006), Standke (2008a), Lustrino & Wilson (2007)

- Oligocene deposits

Middle Eocene to Oligocene sedimentation was terminated by a fall in sea level leading to a renewed erosion around the basin margins (*figure 3b*). It did not last too long until the increase in global temperature in Rupelian times led to rise in eustatic sea level and a widespread transgression of marginal area (Doornenbal and Stevenson, 2010).

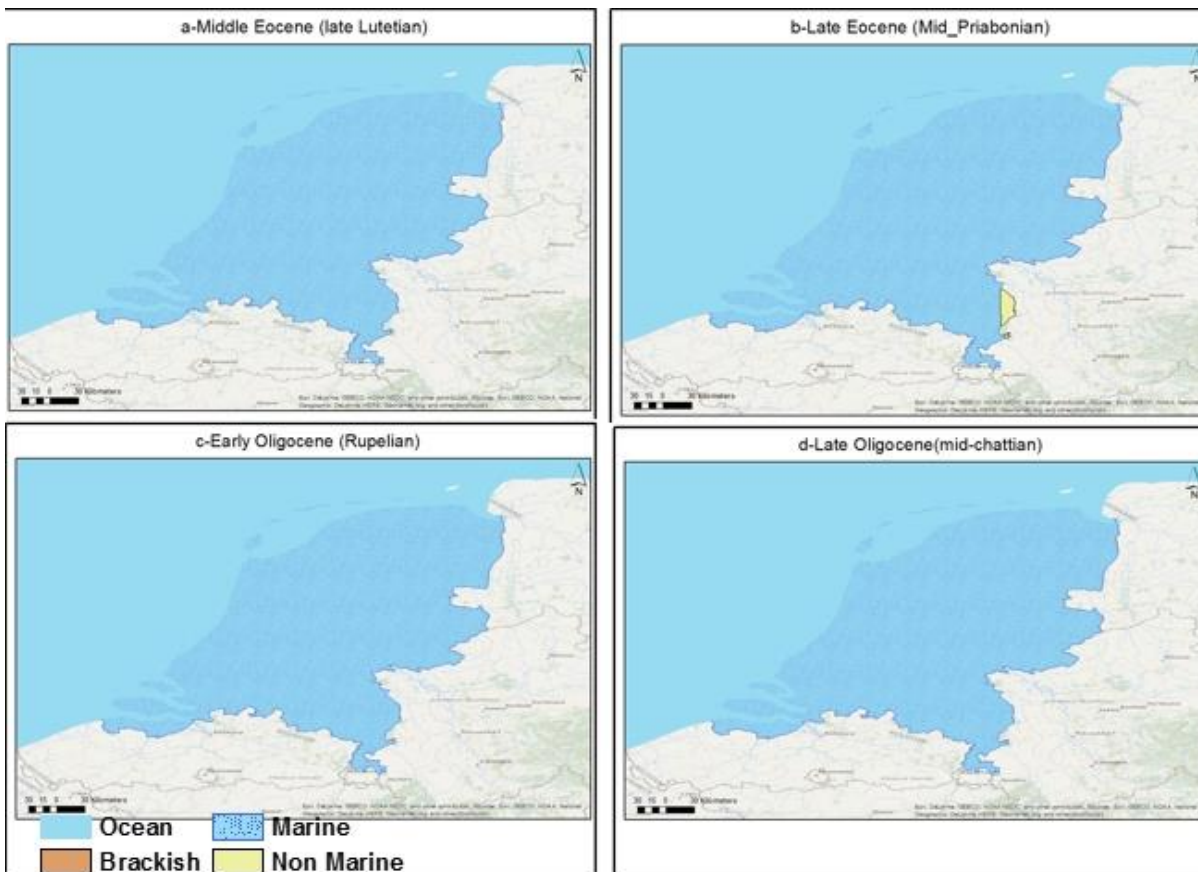


Figure 3: Type of deposits from Mid-Eocene to Late Oligocene-modified

a. Middle Eocene (late Lutetian: 42.5 Ma); b. Late Eocene (mid-Priabonian: 36Ma); c. Early Oligocene (Rupelian: 31 Ma); d. Late Oligocene (mid-Chattian: 26 Ma).

Source: Based on the regional maps of Vinken (1988), Ziegler (1990), Ahmadi et al. (2003) and Jones et al. (2003), together with maps of Lotsch (1969, 2002), Thiry & Dupuis (1998), Martiklos (2002), Piwocki (2004), Gürs (2005), Heilmann-Clausen (2006), King (2006), Standke (2008a), Lustrino & Wilson (2007)

- Miocene to middle Quaternary deposits

In addition to rise and fall in sea level, this period was associated with the development of major river systems that supplies sediment in the western part of the southern Permian basin (Doornenbal and Stevenson, 2010)

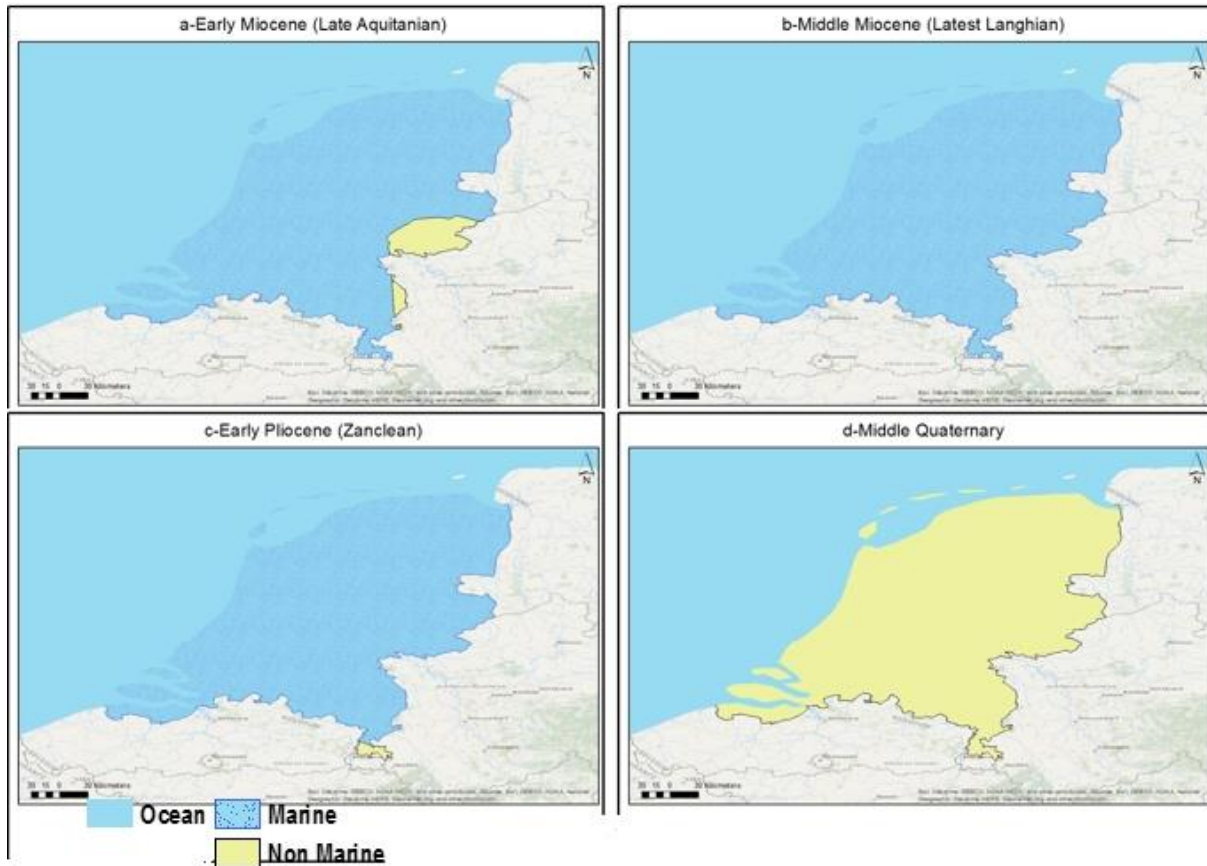


Figure 4: Type of deposits from Miocene to middle Quaternary –Modified

a. Early Miocene (late Aquitanian: 20.5 Ma); b. Middle Miocene (latest Langhian: 14 Ma); c. Early Pliocene (Zanclean: 5 Ma); d. Middle Quaternary

Source: Based on the regional maps of Vinken (1988), Ziegler (1990), Ahmadi et al. (2003) and Jones et al. (2003), together with maps of Lotsch (1969, 2002), Thiry & Dupuis (1998), Martiklos (2002), Piwocki (2004), Gürs (2005), Heilmann-Clausen (2006), King (2006), Standke (2008a), Lustrino & Wilson (2007)

- Pleistocene/Holocene deposits and sea level evolution

In the Pleistocene, the deposits were marine, fluvial and glacial

- Marine: Pleistocene has glacial stages and interglacial stages (*figure 5*). During glacial stages, sea level decreases, so the sea has retreated northwestwards (*figure 6*), however in the interglacial, it advances southwestwards making the Netherlands a coastal area. So when sea level was high, marine deposits were laid down in the west of Netherlands and during period of low sea level, the deposits were terrestrial and interstitial water was fresh as it originated from precipitation or water infiltration from river

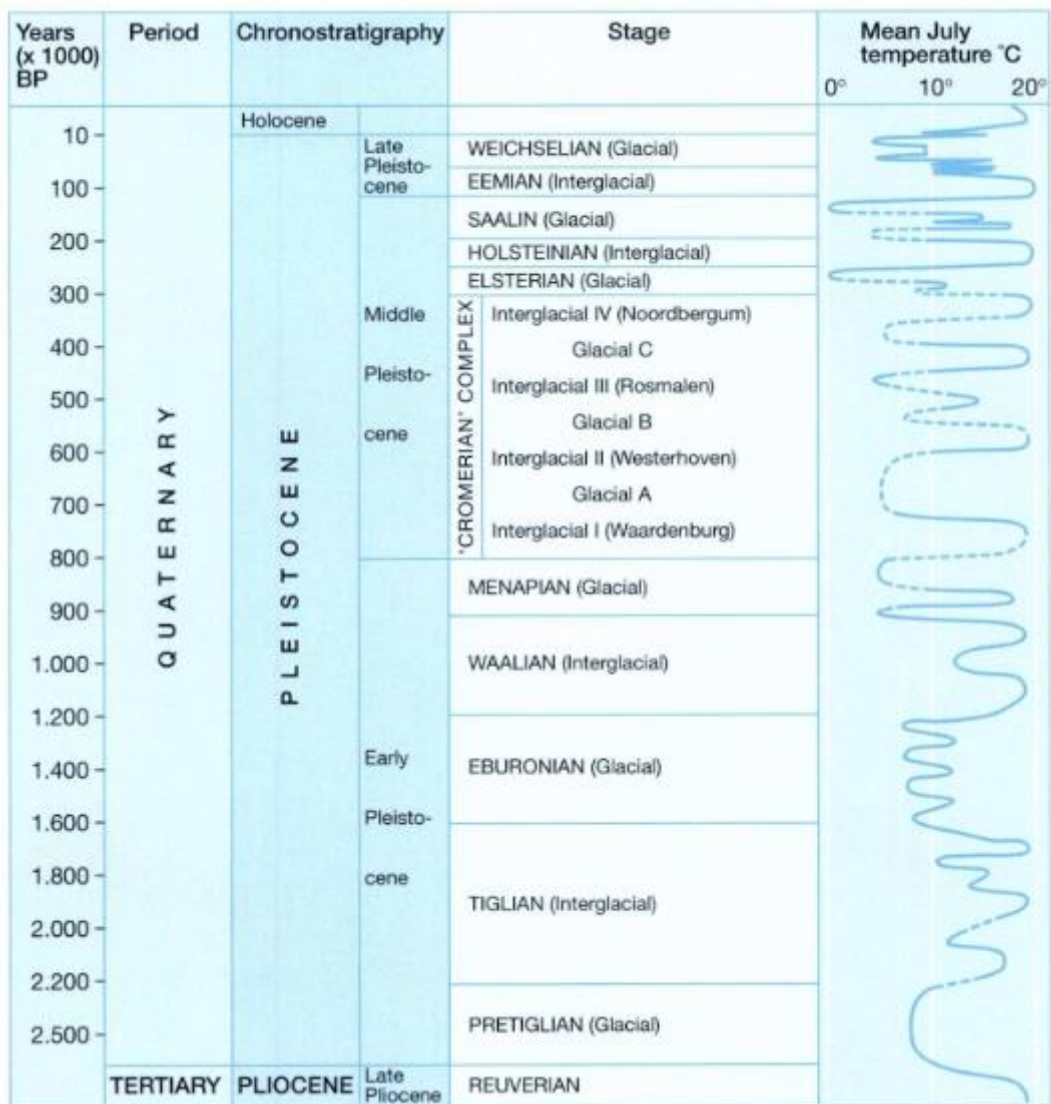


Figure 5: Quaternary chronology and the associated mean July temperatures

Source: Zagwijn and van Staaldin (1975)

- Fluvial deposits

They are found along rivers and are affected by river flow and therefore by colder and warmer periods. They are characterized by coarse and fine layers vertically and big differences in thickness and permeability laterally (Dufour, 1998). They contain fresh pore water and combined with high transmissivity, they are suitable for groundwater abstraction.

- Glacial deposits

They are limited to the north of the country. For example the ice pushed ridges which are important in the hydrogeology of Netherlands (*figure 24*). They are porous and permeable (Dufour, 1998)

During the Holocene, the temperature increased steadily (*figure 5*), leading to melting of ice and rising of sea level. This marine transgression had 3 repercussions: the shoreline migrated southeastwards and then eastwards, deposits laid down in sea or brackish water were poorly permeable and groundwater rises accompanying the sea level rise (Dufour, 1998). Main deposits during the Holocene are coastal dunes which are the most important reserves of fresh water in west of Netherlands, confining peat and clay deposits that determines the interaction between the surface and groundwater in the west and north of Netherlands. The *figure 7* presents a simplified overview of the surface geology of the Netherlands



Figure 6: Coastline extension during Pleistocene/Holocene

Source: (Dufour, 2000)


 Maximum extension of Holocene coastline
 Maximum extension of Early Pleistocene coastline (Maassluis Formation)

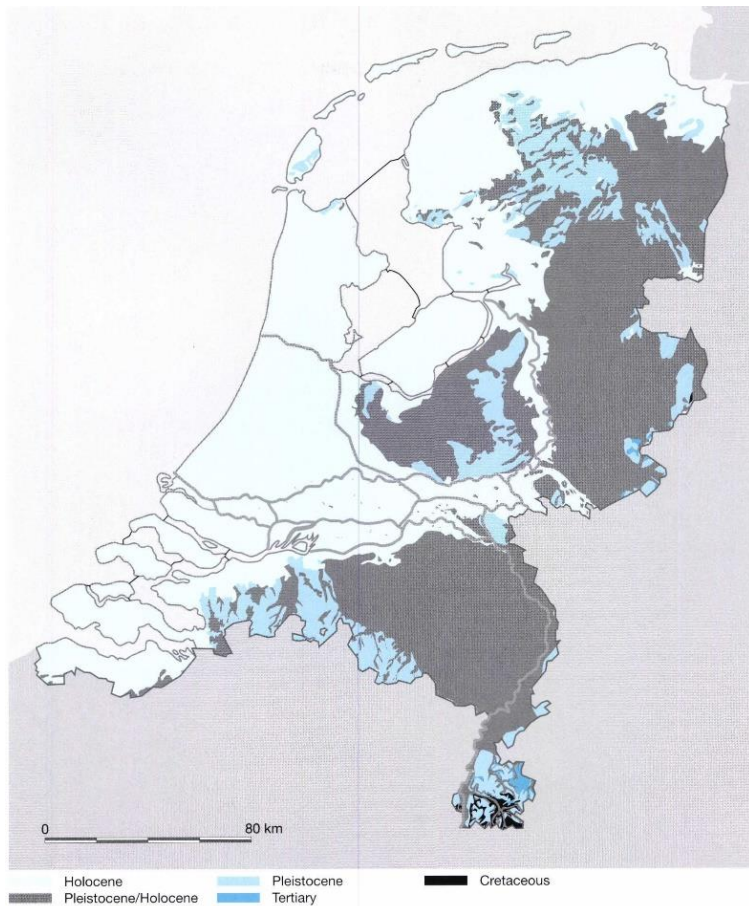


Figure 7: Surface deposits of the Netherlands

Source: (Dufour, 2000)

c. Netherlands Zechstein group

The present thesis focuses in diffusion so a description of the Zechstein group will be needed because it is the source area/point for the salinity. The Zechstein is present over most of the Netherlands, on and offshore (Doornenbal and Stevenson, 2010). It was established by rapid flooding of a late Permian intracontinental topographic depression.

Zechstein deposits are strongly cyclical, consisting of carbonates and mudstones followed by evaporites. The glaciation periods are the origin of this periodicity since it controlled the marine incursions from the Barents Sea (Ziegler, 1990a), in combination with the high evaporation rates.

Traditionally Zechstein consists of four main evaporites layers (Doornenbal and Stevenson, 2010), known as Z1-Werra, Z2-Stassfurt, Z3 Leine and Z4-Aller (figure below)

- Z1-Werra

The Z1 halite is restricted to the peripheral sub-basins to the south of the main basin. Some of these basins have anhydrite intercalations in halite deposits up to several tens of meters thick (Peryt & Kovalevich, 1996)

- Z2-Stassfurt

3 stages of deposition characterize this Zechstein group based on distinct polyhalite marker beds (Geluk et al., 2000). During the two first stages, the topography is influencing the thickness of halite that tends into deeper-water salt complex northwards (succession of halite, polyhalite and carnallite). During the third period, the salt filled most remaining depression in the basin. The Stassfurt and overlying layers have been deformed due to the extensive salt movement. (Doornenbal and Stevenson, 2005)

- Z3 Leine

The formation has a 300m thickness and include the Grey Salt Clay (T3), Platy Dolomite (Ca3), Main Anhydrite (A3) and Younger Halite (Na3), whereas in the southern north sea, the carbonates into fluvial sandstones (Geluk et al., 1997).

- Z4 Aller

The formation consists of claystone - anhydrite - salt sequence in the main basin and sub-basins, and a claystone - sandstone along the basin margin (van Adrichem Boogaert and Kouwe, 1993)

- Z5 Ohre

This is presumed the youngest formation and consists of claystone and rock salt. The formation is present only in areas where Z4 is fully developed.

It is also good to mention that the present day thickness of the Zechstein does not relate with the original thickness of Zechstein deposits and this is due essentially to widespread post-Permian salt movement and erosion. (Doornenbal and Stevenson, 2005)

Z5 (Ohre) Formation	
Z4 (Aller) Formation	Z4 Salt
	Pegmatite-Anhydrite
	Red Salt Clay
Z3 (Leine) Formation	Z3 Salt
	Main Anhydrite
	Z3 Carbonate
	Grey Salt Clay
Z2 (Stassfurt) Formation	Z2 Roof Anhydrite
	Z2 Salt
	Basal Anhydrite
	Ca2 Carbonate
Z1 (Werra) Formation	Z1 Anhydrite
	Z1 Carbonate
	Coppershale

Figure 8: Zechstein layers

Source: (Doornenbal and Stevenson, 2010)

d. Wells

Several wells (more than 6310) were drilled in Netherlands on and offshore for oil and geothermal energy. In the present works 3 wells were used AST02, AST01 and NDW. They are drilled in the Roer valley graben (*figure 9*)

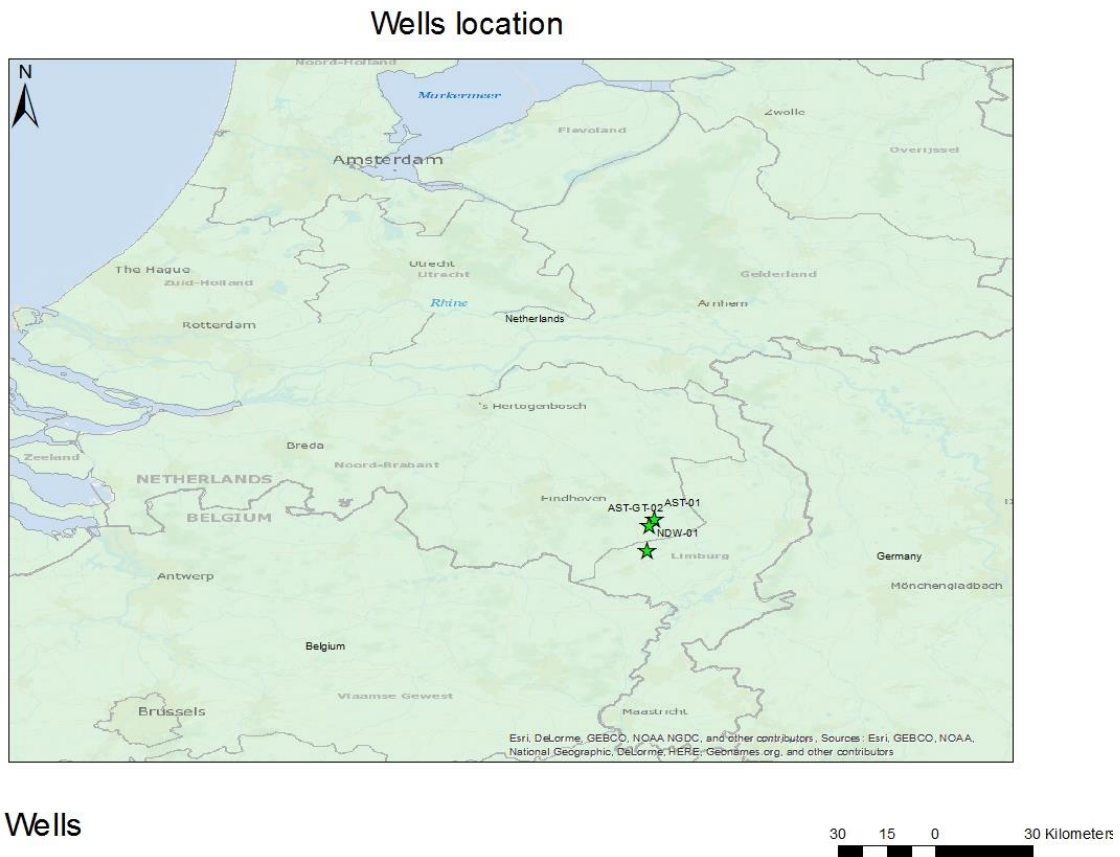


Figure 9: The location of wells AST, NDW used to construct input files

Name	Lat/Long (°)ED50	TVD (m)	Additional information
AST-02	51.38088806 N, 5.7764057 E	1673	
AST-01	51.39659558 , 5.79092257	2664	2 km north east of AST-02
NDW-01	51.31160526 , 5.77072472	2942	7.5 km south of AST-02

Table 1: Location and Total vertical depth of the Wells AST-01, AST-02 and NDW-01

2. Solute diffusion

The solute diffusion within the subsurface is controlled by several physical factors, some of these factors are:

- Particle molecular weight: Diffusion is a result of molecular motion. Human can push a wheelbarrow much faster than a car, therefore using the same amount of force, larger molecules will diffuse slower than smaller ones.
- Temperature: As the temperature increase, the available energy for molecules to move is bigger. Thus the rate of diffusion will be faster as the temperature is increasing.
- Concentration gradient: The greater the difference in solute concentration between two points in the subsurface, the faster the substance will diffuse.
- Surface area: When diffusing between two compartments, the larger is the surface area delimitating these compartment, the greater is the rate of diffusion.
- Pores permeability connection: If pores are badly connected, then diffusion through them is very low. The more permeable the porous surface is, the faster is the diffusion.

Diffusion in groundwater is described by the Fick's law, which say that chemical mass flux (diffusion flux) is proportional to the concentration gradient in a fluid and molecular diffusion coefficient (molecules moves towards a zone of lower concentration).

It is described by the Fick's first law: (equation 1)

$$F = -D_w * \frac{dC}{dx} \quad (1)$$

Where F is the diffusive flux, D_w is the coefficient of molecular diffusion in free water, C is the concentration of the molecules/ions and x is the direction along the concentration gradient. The coefficient of molecular diffusion is ion and temperature dependent. They show a general trend of decreasing with both increasing charge and decreasing ionic radius (Ingebritsen et al., 2006) (*figure 25* in appendix).

In a porous medium the coefficient of molecular diffusion must be expressed in different term since there is instead of free path, a solid somewhere that restrict, decrease the area available for molecules to diffuse and increases the distance over which the solute must diffuse. GreenKorn and Kessler (1972) express the coefficient of diffusion in porous medium D_m as a function of effective porosity n_e and tortuosity τ described by the following equation (2):

$$D_m = \frac{n_e}{\tau} * D_w \quad (2)$$

Where the tortuosity is expressed by Millington-Quirk (Sanchez et al., 2003) as

$$\tau = n^{-\left(\frac{1}{3}\right)} \quad (3)$$

In this study the diffusion will be applied in geological process. As it has been discussed earlier in equation 2, D_m is affected by porosity and tortuosity therefore D_m is always less than D_w .

Typical diffusion coefficients (D_w) for geological process range from 10^{-11} to 10^{-10} m^2/s (Ingebritsen et al., 2006).

The change in solute concentration in the subsurface over time is described by the second law of Fick's law that combines first Fick's law with a mass balance equation:

$$- n_e * \frac{\partial C}{\partial t} = \frac{\partial}{\partial x} \left(D_m * \frac{\partial C}{\partial x} \right) \quad (4)$$

This equation assumes that effective porosity does not change over space and time and the diffusion coefficient does not vary with respect to space or concentration (Ingebritsen et al., 2006)

$$- n_e * \frac{\partial C}{\partial t} = D_m * \nabla^2 C \quad (5)$$

Where ∇^2 is the second derivative over x, y, z.

III. Methods and materials

1. Resistivity to pore water salinity

Salinity dataset can be used as input for the diffusion model, one idea was to derive it from resistivity log from boreholes (NL Oil and Gas Portal, 2015a) and compare it with direct measurement of the salinity of deep groundwater (Heederik et al., 1988)

The first step is to derive an expression for water resistivity (R_W).

According to Archie's law (Crain, 2006):

$$F=R_0/R_W =A/n ^M \quad (6)$$

Where F is formation resistivity factor (unitless), R_0 is the resistivity of rock filled with 100% water (ohm-m), R_W is the water resistivity (ohm-m), M is the cementation factor (unitless and depends on rock type and varies from 1.3 to 2.6 (Crain, 2006)), n is the porosity (unitless) and A is the tortuosity (unitless) (we assume A=1 in all the simulation)

Equation (6) lead to:
$$R_W= A/ (R_0* n ^M) \quad (7)$$

To compute this equation, the well is AST-GT-02 is used. From the attribute table of this well in the website (NL Oil and Gas Portal, 2015b), it's stated that it's a water well, therefore the estimation of $R_0 =R_T$ (R_T is the rock resistivity filled with water and oil) can be made.

The choice of resistivity log is between deep induction resistivity log “**ILD,ohm-m**” and medium induction resistivity log “**ILM,ohm-m**” log. ILD is chosen because it gives resistivity of the uninvaded zone (no alteration due the drilling mud) (DUNHAM, LANNY, Consulting Petrophys, 2001).So $R_0 =$ ILD and this value is replaced in the equation (7) :

$$R_W= A/ (ILD* n ^M) \quad (8)$$

- A second step is to calculate the porosity needed in equation 8

To get the porosity, the density log RHOB is used, as density is proportional to the porosity. RHOB log is available from the composite file for some wells in the Netherlands geological website (NLOG). The porosity is calculated for different depth using the equation below:

$$n = (\rho_m- \rho_b)/ (\rho_m- \rho_w) \quad (9)$$

Where ρ_m is the density of the matrix (mean value of 2650 kg/m³), ρ_b is the bulk density (from RHOB log) and ρ_w is the density of water (1025 kg/m³)

Next is the calculation of the water resistivity in equation (8).3 resistivities are considered depending on 3 cementation values

$$\color{red}{\oplus} \color{blue}{\oplus} \color{green}{\oplus} \quad M=1.3$$

$$\color{red}{\oplus} \color{blue}{\oplus} \color{green}{\oplus} \quad M=2.6$$

$$\color{red}{\oplus} \color{blue}{\oplus} \color{green}{\oplus} \quad M=1.8$$

- The third step is to calculate the pore water salinity from water resistivity

Water resistivity can be converted to salinity in ppm NaCl at any temperature (Crain, 2006)

$$W_s = 400000 / T(F) / (R_w^{1.14}) \text{ in ppm NaCl} \quad (10)$$

Where W_s the water salinity (ppm NaCl) and T is temperature in Fahrenheit provided in NLOG website for every well.

The salinity is then calculated from this equation from the 3 resistivities

Now that the calculated salinity is computed, the measured one is needed.

- The final step is compute the measured salinity from the chloride concentration

The Dutch geological survey has provided chloride concentrations for **AST-02** well for different depths ranging from 630 meters until 1465 meters. These chloride concentrations have been converted to salinities using the formula provided by Vernier Software (2016)

- **Salinity (ppt) = 0.0018066 * [cl-](mg/l) (11)**

2. Single well diffusion model

a. Model code

For the single well diffusion, the Pybasin model is used (Luijendijk et al., 2011). It models burial and temperature history. Burial history is calculated by decompacting present-day stratigraphic thicknesses of units, and thermal history is based on 1D heat conduction with a specified heat flux at the base of the sediments and a specified surface temperature. Solute diffusion was added to Pybasin to cover also the solute diffusion. An exhumation period starting at 70Ma and finishing at 85.8 Ma was used. It's stated in the same journal (Luijendijk et al., 2011) that the exhumation in the Netherlands does not exceed 1000 m and it's somewhere

between 0 and 500m for RGV basin. Hence, the exhumation magnitude is assumed to be 500 meter.

The model has several input files:

- The lithological properties file of the study area for example: sand, silt, clay...
For each lithological element, the density, surface porosity, compressibility, thermal conductivity and heat production are specified.
- Salinity data for every well: represents measured salt concentration at specified depth.
- Stratigraphy information file:describes all the stratigraphically units that exist in the RVG basin with bottom and top age, origin, and percentage of lithological elements, for example :

Table 2: Preview of the stratigraphy information file used as input for Pybasin model

Strat_unit	Age_bottom	Age_top	Conglomerate	Sand	Silt	Clay	Carbonate	Anhydrite	Halite
Quaternary	1.8	0	0.45	0.45	0	0.1	0	0	0
OMM	19	17.25	0.1	0.72	0.05	0.05	0.08	0	0

- Surface salinity file:marks out the surface salinity from the present day and going backward to 300 million years ago.
- Surface temperature file:outlines the surface temperature from the present day, and going backward to 300 million years ago.
- Well stratigraphy file:give a detailed account of the well composition strata (Table 3)

Well	Depth_top	Depth_bottom	Strat_unit
TestWell 1	0	175	NUCT
TestWell 1	175	340	NUKO
TestWell 1	340	778	NUBAU
TestWell 1	778	857	NUVIH
TestWell 1	857	940	NUBAL

Table 3: well stratigraphy file for TestWell 1 used as input for Pybasin model

For more details about the strata coding please refer to van Adrichem Boogaert (1993)

The model has 4 main modules:

- Pybasin.py=Main entry to the program (read input file, formatting,...)
- Pybasin_lib.py=Main script, functions, for solving all the equations
- Pybasin_params.py: all model parameters (Boundary condition, diffusion...)
- Model_Scenario.py: specify all scenario/well that will be run in one go.

The figure below represents the mechanism used by Pybasin program. It's recommended that the user will only modify Pybasin_parms and Model_Scenario files to specify his preferences

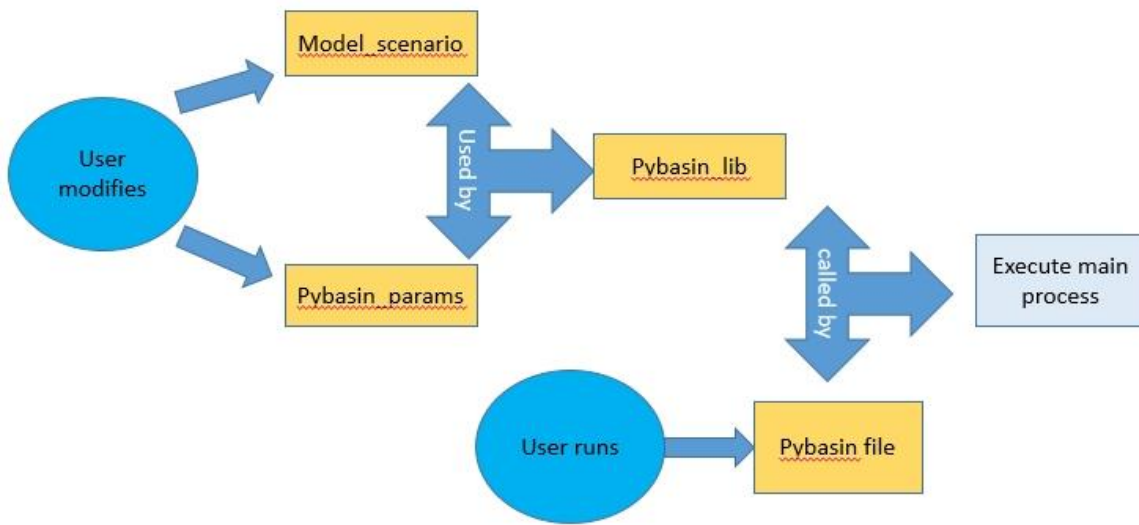


Figure 10: Model-code run-time

The model code solve the Fick's second law numerically: $-n_e * \frac{\partial C}{\partial t} = D_m * \nabla^2 C$ (5). The porosity is calculated at every depth using the (Athy, 1930) equation:

$$n = n_0 * e^{-cz} \quad (6)$$

It is used also to determine the thickness of the pore space and finally the total thickness of the strata (pore space + matrix). The model solve the equation (5) using the finite difference method (FDM).It is a numerical method that approximates derivative by combining nearby function values using a set of weights (Courant et al., 1928).For example the derivative of concentration versus time $\frac{dC}{dt}$ can be approximated with a forward finite difference approximation as :

$$\frac{\partial C}{\partial t} = \frac{C_i^{n+1} - C_i^n}{t^{n+1} - t^n} = \frac{C_i^{n+1} - C_i^n}{\Delta t} = \frac{C_i^{new} - C_i^{current}}{\Delta t} \quad (7)$$

Molecular diffusion coefficient is ion dependent and affected by the temperature. Since the interest is in brine transport, and in deep formation, then the temperature varies considerably. Hence, estimating the diffusion coefficient of chloride ion at different temperature is essential and preliminary part of the model.

In different literature, the diffusion coefficient of chloride in free water D is $20.3 * 10^{-10} m^2/s$ at 25 degree Celsius (Ingebritsen et al., 2006).

Simpson and Carr (1958) have shown that temperature dependence of viscosity and self-diffusion of water in the temperature range 0-100 °C can be adequately described by Stokes-Einstein relation, it means:

$$\left(\frac{D*\mu}{T}\right)_{T_{ref}} = \left(\frac{D*\mu}{T}\right)_{T_{cal}} \quad (8)$$

Where D is the molecular diffusion ($\frac{m^2}{s}$) coefficient, T is the absolute temperature (K), μ is the water viscosity (cP), T is the absolute temperature.

- The term **Ref** in equation 8 refers to all values of reference (at 25 °C), for example
 - ✓ $T_{ref} = 298.15 K$
 - ✓ $D_{ref} = 2.03 * 10^{-9} m^2/s$
 - ✓ $\mu_{ref} = 0.890 cP$ (Kuo, 1999)
- The term **Cal** (equation 8) refers to the calculated or new values.

So from equation 8 it can be deduced that

$$D_{T_{cal}} = \left(\frac{D*\mu}{T}\right)_{T_{ref}} * \left(\frac{T}{\mu}\right)_{T_{cal}} \quad (9)$$

From equation 9, it can be noticed that in order to calculate the molecular diffusion at any temperature, the viscosity of water at the same temperature is first required.

Kestin et al (1981) developed several relationships to describe the viscosity. The equation below from Batzle and Wang (1992) approximates the viscosity at temperature below 250 °C:

$$\mu = 0.1 + (0.333 * S) + (1.65 + 91.9 * S^3) * \exp[-(0.42 * (S^{0.8} - 0.17)^2 + 0.045) * T^{0.8}] \quad (10)$$

- ✓ S =salinity in ppm
- ✓ T =Temperature in degree Celsius

Equation 9 and 10 are scripted and added to pybasin-lib in order to calculate the chloride diffusion coefficient at every temperature. The model grid size was set to 100m and time step to 100 000 year.

It is required to mention that the model domain is a 1D model with no flow boundary condition at the right and left and Dirichlet boundary at the bottom and top. The salinity concentration is set to:

- Bottom boundary: value that exceeds 0.3kg/kg (halite saturated) (Hanor, 1994). Zhang et al. (2013) have stated that during the formation of Zechstein salt, the halite starts to precipitate when the salinity of seawater reached 10 to 12 times of the normal seawater (0.035kg/kg), it means 0.34 kg/kg to 0.42 kg/kg. So **0.40 kg/kg**, a middle value is taken during the simulation.
- Fresh water boundary: 0.0001kg/kg (Dufour, 1998)
- Sea water salinity: 0.035 kg/kg

The bottom boundary condition is set by Pybasin to the top of the salt member (Zechstein group) (at the bottom of the overlying claystone member.)

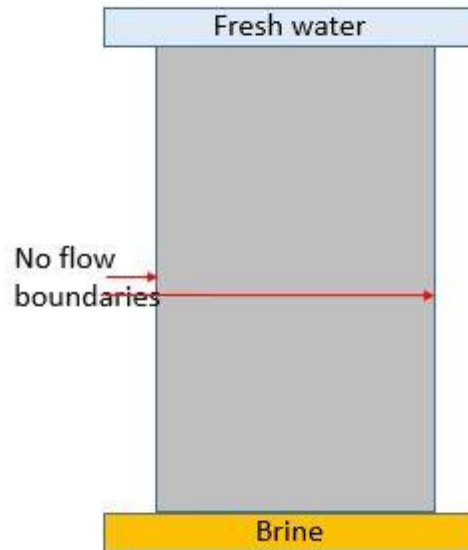


Figure 11: Model domain

For any user who wants to start the model, he should set up the values (salinity, wells name, fixed salinity, exhumation period, exhumation magnitude,).

b. Input well

The model input files include a well stratification file that should be prepared because well AST-02 has not been drilled deeper than the Cretaceous group. The depth of the underlying formations until the base of the salt were estimated. The Permian Zechstein group have been estimated using data from well AST-01 and NDW-01 and available thickness data based on seismic interpretations (NL Oil and Gas Portal, 2015a)

Well AST-01 (table 8 in the appendix) has been used to estimate the thickness of Upper Germanic Trias and Lower Germanic Trias formations. Since the distance between the two wells is not that big to have big difference in lithology, it is assumed during the present work that the thickness percentage of each formation in the Triassic period is almost the same between the two wells. And therefore, the well AST-02 will be extended through the Triassic period.

Then the well NDW-01 (stratification table 5 in appendix) is used to estimate the Zechstein formation thicknesses. The same assumption about thickness percentage that correlate well AST-02 and AST-01 is made for the well AST-02 and NDW-01.

The following table represents the final stratigraphy of well AST-02 that has been used by the model.

Group	Formation/Member	Depth_top	Depth_bottom	Strat_code
Quaternary		0	175	NUCT
Upper North Sea NU	Kieseloolite Formation	175	340	NUKO
	upper Breda member	340	778	NUBAU
	Heksenberg Member	778	857	NUVIH
	lower Breda member	857	940	NUBAL
Middle North Sea NM	Someren member	940	992	NMVFS
	Veldhoven Clay Member	992	1173	NMVFO
	Voort Member	1173	1401	NMVFV
	Steensel Member	1401	1415	NMRFT
	Rupel Clay Member	1415	1494	NMRFC
	Vessem Member	1494	1513	NMRFS
Lower North Sea NL	Reusel Member	1513	1558	NLLFR
	Landen Clay Member	1558	1586	NLLFC
	Gelinden Member	1586	1606	NLLFG
	Heers Member	1606	1632	NLLFS
	Swalmen Member	1632	1635	NLLFL
Chalk CK	Houthem Formation	1635	1673	CKHM
Altena AT	Aalburg Formation	1673	1989	ATAL

	Sleen Formation	1989	2002	ATRT
Upper Germanic Trias RN	Keuper Formation	2002	2063	RNKP
	Muschelkalk Formation	2063	2192	RNMU
	Rot Formation	2192	2431	RNRO
	Solling Formation	2431	2452	RNSO
Lower Germanic Trias RB	Hardegsen Formation	2452	2524	RBMH
	Detfurth Formation	2524	2575	RBMD
	Volpriehausen Formation	2575	2735	RBMV
	Lower Buntsandstein Formation	2735	2915	RBSH
Zechstein ZE	Zechstein Upper Claystone Formation	2915	2927	ZEUC
	Z3 Carbonate Member	2927	2937	ZEZ3C
	Grey Salt Clay Member	2937	2939	ZEZ3G

Table 4 : Stratification of input well AST-02 after extension

The model was run for a constant diffusion coefficient and with variant diffusion coefficient

3. Modelling diffusion for multiple synthetic wells

The 1D diffusion model was used here for the salinity mapping of whole Netherlands. To have a salinity output for Netherlands, input wells data are needed to apply the diffusion model.

Well stratigraphy and stratigraphy info are two input files that are directly related to wells in the diffusion model. Therefore these two files must be modified. Instead of describing depth top and depth bottom of every formation, it will be more depth top and depth bottom of every group (a group is a set of formation, Table 4) or two successive group due to data limitation

Geological survey of the Netherlands's website provides digital geological model of the deep subsurface of the Netherlands (NL Oil and Gas Portal, 2015a) that were used to derive necessary data for the wells. It's a subsurface raster catalogue layer covering on-and offshore of the Netherlands.

The following files are used to estimate the thickness of these layers at every well.

- Thickness of the Upper North Sea groups (NU)
- Thickness of the Lower and Middle North Sea groups (NL+NM)
- Thickness of the Chalk Group (CK)
- Thickness of the Rijnland Group (KN)
- Thickness of the Niedersachsen and Schieland groups (SL)
- Thickness of the Altena Group (AT)
- Thickness of the Lower Germanic Trias Group (RB+RN)

Once, the files are available, georeferenced, a script using Arcpy (figure 26 in appendix) was developed to automatize the work flow: The script main functionalities are:

- Creating wells within a regular grid distance defined by the user (2km*2km)
- For every well created:
 - Assign the thickness of the geological group (figure 13)
 - Compute the depth top and depth bottom of the geological group
 - Check the surface origin (marine, on marine, brackish) for every geological time scales
- Export the results to CSV files that adapts to the Pybasin code input format

At the end of the script, **10573** well are created within the Netherlands, with all necessary data needed to run the model.

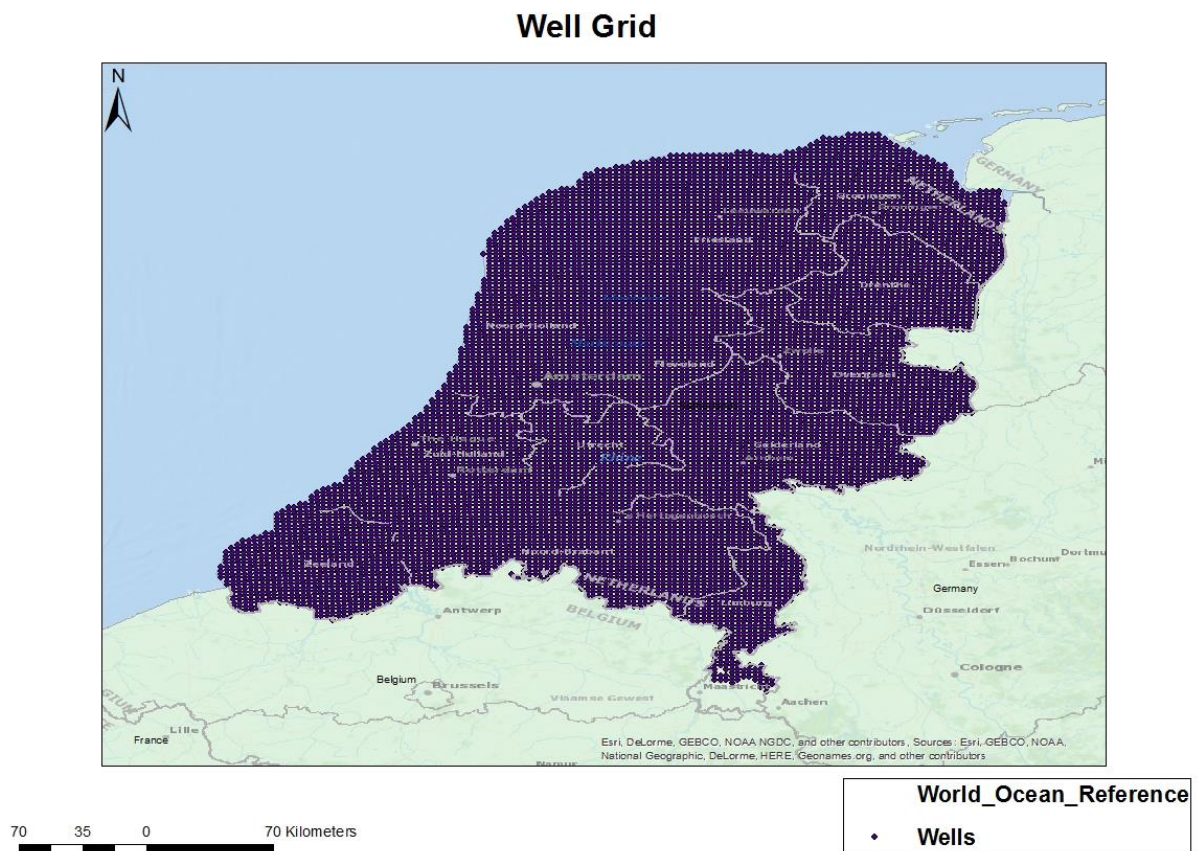


Figure 12: Synthetic salinity wells created from digital geological maps of the Netherlands

Wells																			
FID	Shape *	Id	Name	Thick_NU	Thick_NMNL	Thick_CK	Thick_KN	Thick_SL	Thick_AT	Thick_RNRB	Top_NU	Bottom_NU	Top_NMNL	BottomNMNL	Top_CK	Bottom_CK	Top_KN	Bottom_KN	Top_SL
0	Point	0	Well198	52.87	330.11	136.63	0	0	0	0	0	52.87	52.87	382.98	382.98	519.61	519.61	519.61	519.61
1	Point	0	Well199	52.78	345.37	141.75	0	0	0	0	0	52.78	52.78	398.15	398.15	539.9	539.9	539.9	539.9
2	Point	0	Well200	52.72	360.96	146.66	0	0	0	0	0	52.72	52.72	413.68	413.68	560.34	560.34	560.34	560.34
3	Point	0	Well201	52.85	376.68	151.6	0	0	0	0	0	52.85	52.85	429.33	429.33	580.93	580.93	580.93	580.93
4	Point	0	Well356	53.17	307.19	130.13	0	0	0	0	0	53.17	53.17	360.36	360.36	490.49	490.49	490.49	490.49
5	Point	0	Well357	53.1	321.41	136.53	0	0	0	0	0	53.1	53.1	374.51	374.51	511.04	511.04	511.04	511.04
6	Point	0	Well358	53.04	336.29	142.57	0	0	0	0	0	53.04	53.04	389.33	389.33	531.9	531.9	531.9	531.9
7	Point	0	Well359	52.96	351.62	148.07	0	0	0	0	0	52.96	52.96	404.58	404.58	552.65	552.65	552.65	552.65
8	Point	0	Well360	52.91	367.26	153.2	0	0	0	0	0	52.91	52.91	420.17	420.17	573.37	573.37	573.37	573.37
9	Point	0	Well361	53.48	382.45	158.32	0	0	0	0	0	53.48	53.48	435.93	435.93	594.25	594.25	594.25	594.25
10	Point	0	Well362	56.59	395.17	163.82	0	0	0	0	0	56.59	56.59	451.76	451.76	615.58	615.58	615.58	615.58
11	Point	0	Well363	59.75	407.71	170.05	0	0	0	0	0	59.75	59.75	467.46	467.46	637.51	637.51	637.51	637.51
12	Point	0	Well364	63.14	420.07	177.43	0	0	0	0	0	63.14	63.14	483.21	483.21	660.64	660.64	660.64	660.64
13	Point	0	Well365	66.21	432.56	187.21	0	0	0	0	0	66.21	66.21	498.77	498.77	685.98	685.98	685.98	685.98
14	Point	0	Well513	54.56	276.15	114.97	0	0	0	0	0	54.56	54.56	330.71	330.71	445.68	445.68	445.68	445.68

Figure 13: The thickness of synthetic wells at every group of strata

At the end the diffusion model run throughout the 10573 wells with a model grid size of **100 m** and time step of 100000 years producing diffusion results at every 2km.

These results were interpolated using Kriging interpolation (Noel, 1990) and compared to maps of subsurface salinity by Stuurman et al. (2006).

IV. Results and discussion

1. Resistivity to pore water salinity

a. Results and discussion

The calculated salinity using equation **10** has to be compared to the measured one provided by the geological survey of the Netherlands (TNO) (calculated using equation **11**).

The following table summarizes the results:

depth_AH	TNO Salinity ppm	Salinity (M=1.3) ppm NaCl	Salinity (M=2.6) ppm NaCl	Salinity (M=1.8) ppm NaCl
630	2348.58	2630.74466	558.2031955	1449.180221
711	1264.62	2341.981061	550.1290331	1341.573912
795	1083.96	1748.470783	436.9893749	1025.764824
800	1625.94	1864.635779	450.1279948	1079.411633
805	1264.62	1530.581848	360.294065	877.4884026
810	903.3	1559.222869	379.1238589	905.1185652
817	1264.62	1597.333143	378.486982	918.0754323
824	1445.28	1557.834987	389.0919399	913.6976816
880	1083.96	938.1151863	152.8710873	466.8806277
904	11020.26	1047.841032	197.803271	551.836017
905	9033	959.2647555	177.4432477	501.2587257
980	1445.28	1000.329979	175.8601126	512.5873967
997	2529.24	2527.240602	452.8691229	1304.560813
1425	25807.281	634.0471809	69.69236704	271.206378
1429	9755.64	1396.007542	200.9147435	662.352713
1430	24660.09	652.9995439	73.18944794	281.4165565
1435	17135.601	630.2761414	72.21895267	273.9391267

1440	20423.613	764.4073724	113.6894234	367.2952631
1445	19926.798	761.350278	113.2620195	365.8602268
1450	53294.7	860.3027394	142.3693085	430.7014488
1465	9033	1277.07716	279.4052885	711.8323297
1470	7768.38	1691.460317	380.6287145	953.0665994
1470	26015.04	1691.460317	380.6287145	953.0665994
1475	15211.572	1411.136103	312.3078892	790.0439121
1480	10198.257	977.3997292	160.4386687	487.7982388
1482	22076.652	717.9014048	84.8011066	315.6975653
1484	33060.78	610.3101464	67.16064406	261.1689002
1492	39203.22	664.0709035	77.91966624	291.2754793
1510	37938.6	1043.473501	190.7070856	542.739207
1514	46068.3	677.7171089	79.33004796	296.986446
1521	44442.36	970.3942488	138.6121618	459.083541
1522	62689.02	901.4514715	121.5645464	417.1333214
1532	47874.9	685.8230668	76.43963169	294.9270366
1540	76238.52	622.9293676	65.30908396	261.6504078
1545	61063.08	480.348061	38.95909655	182.7935969

Table 5: Comparison between calculated salinities (for different cementation factor) and the measured one by TNO

The calculated salinities are really low if they are compared with the ones measured by the TNO. The error is moderate in shallow formations, but there is a significant underestimation of salinity starting from the depth of 1000m (figure 14)

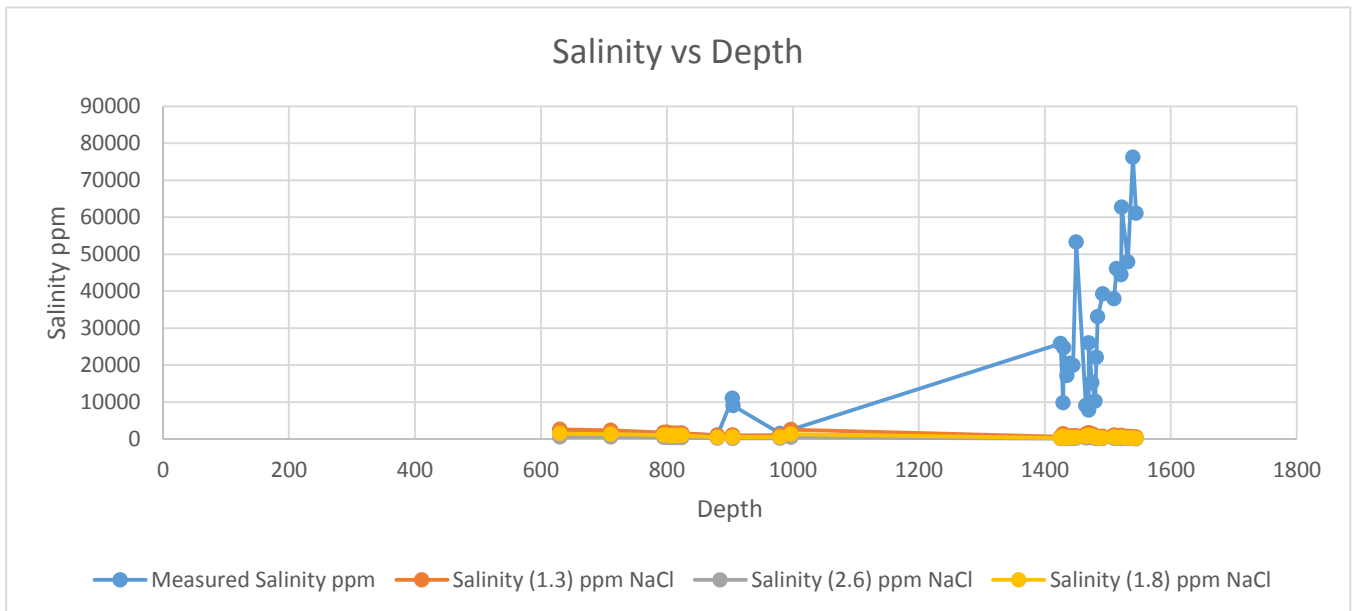


Figure 14: Comparison of calculated salinity using resistivity log data with observed salinity data in well AST-02

There are 3 suppositions for the error that may lead to this difference in salinities:

- The relation followed to for conversion have some weakness somewhere.
- The resistivity data used are not correct

So trying to clarify which probability is more solid, the following conclusion were made:

The followed methods for conversion that I used were implemented in so many petroleum reports so the probability that the error comes from the relation is low. On the other hand, it can be from resistivity data. In order to assess, the idea of comparing the ILD log with the measured salinity is a good option. The summarizing table 7 is attached in the appendix and the figure bellow presents the result

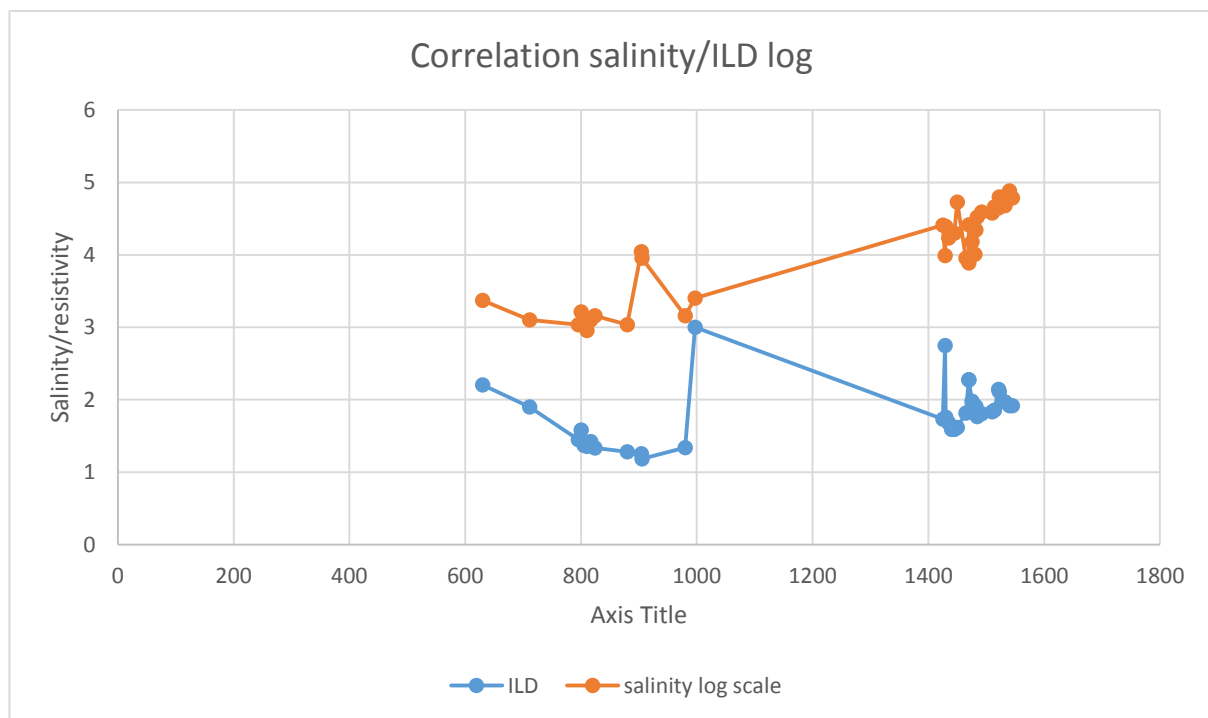


Figure 15: Comparison of resistivity log ILD with measured Salinity for well AST-02

From the figure above, The ILD does not match the salinity before 1000m and after 1400. There is a trend in the interval [1000-1400] m that show when ILD decrease salinity increase and this is logic.

Since the ILD does not give uniformly trend throughout the depth interval, it might be that the raw well log file was processed without some kind of correction, the thing that is hard to testify.

As a conclusion the first part of this project that normally would have provided salinity data from resistivity logs for the available wells in the Netherlands is not trustful, so in order to have logical results at the end, only the measured salinity of well AST-02 will be used in the modelling part since it is the only reliable source available.

2. Diffusion model

a. Single well diffusion

i. Results

Figure 16 shows the result of the diffusion model for borehole AST-02 in the Roer Valley Graben (RVG) for two cases, one with a fixed diffusion coefficient of $20.3 \times 10^{-10} m^2/s$ and one with a variable temperature-dependent diffusion coefficient calculated using the equation 7. The model grid size was set to 100m and time step to 100 000 year

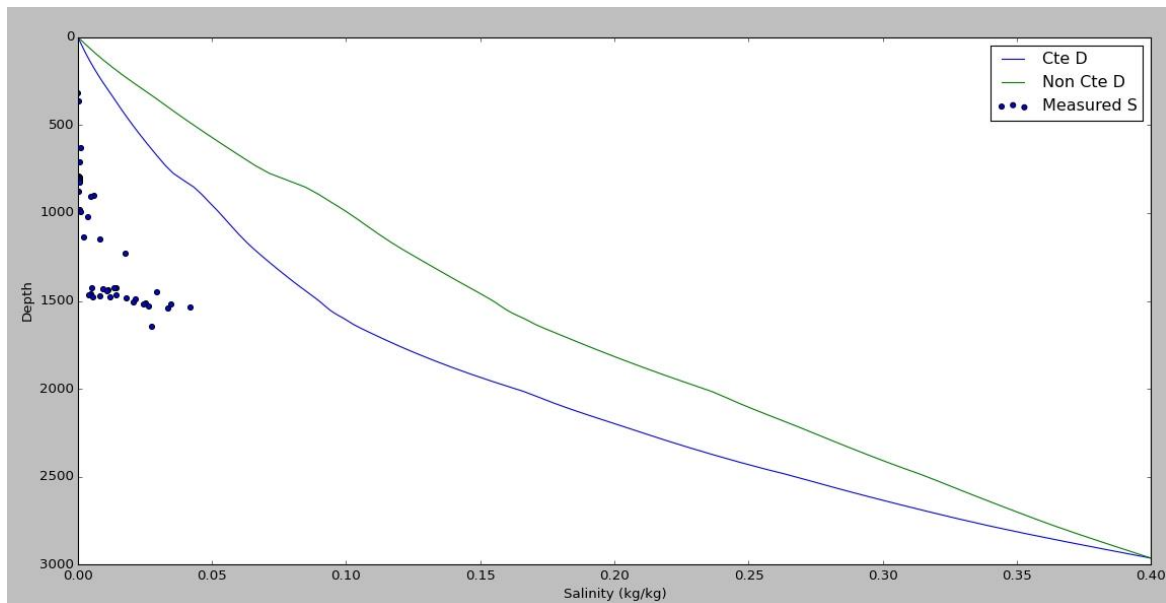


Figure 16: Result of the diffusion model for a fixed and variable diffusion coefficient

Blue line: Salinity concentration using a constant diffusion coefficient

Green line: Salinity concentration using a temperature dependant diffusion coefficient

Scattered plot: observed salinity

The figure below (figure 17) is an exhaustive result of the diffusion model of borehole AST-02 in the RVG. It summarizes the burial and salinity history of this borehole, the present observed salinity and the modeled one. It also indicates how the surface salinity was changing over the last 250 Ma.

The modeled salinity graph values in the figure 17 are 100 times higher than the measured ones (Heederik et al., 1988). The comparison can only be made until the depth of 1646 meters due to the measured data availability.

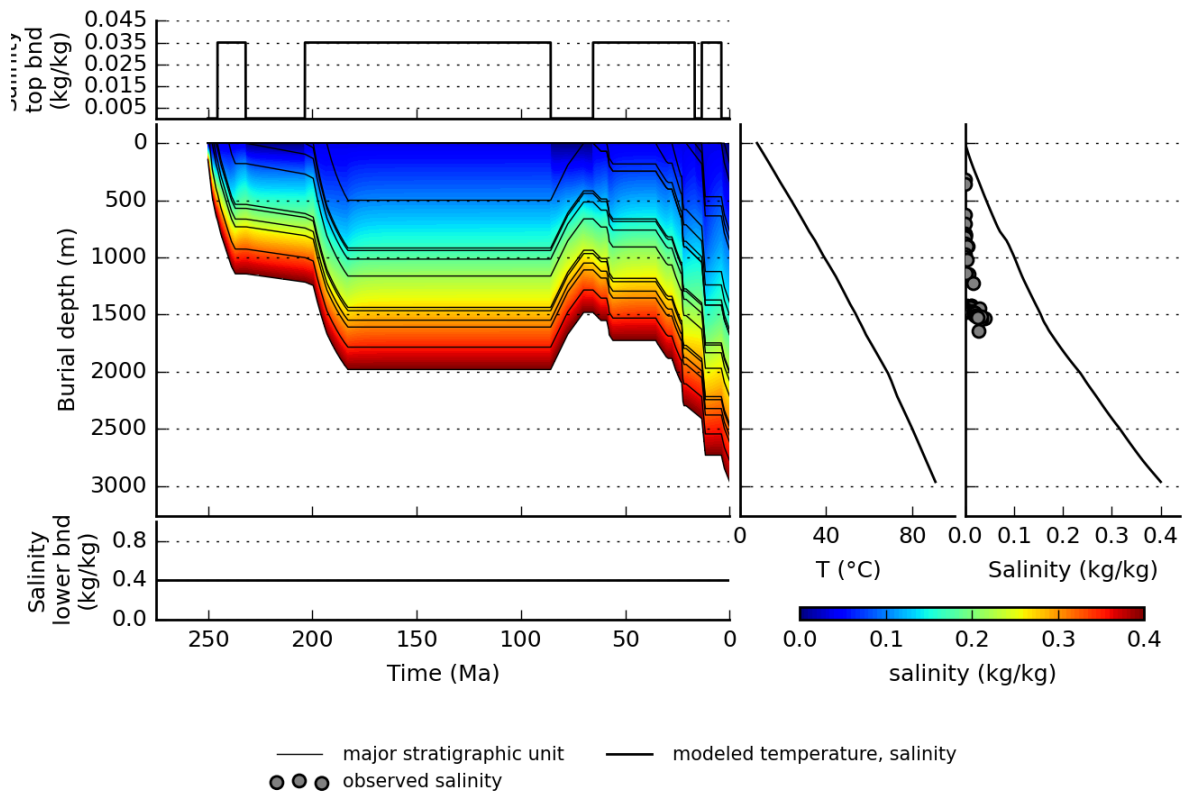


Figure 17: Results of Pybasin model: Burial history and salinity output for borehole AST-02

ii. Discussion

It's shown from the figure 16 that diffusion process using a temperature-dependent diffusion coefficient is faster. This is the logical scenario that occurs in deep sedimentary basins where temperature affects diffusion process. Therefore in all upcoming simulations, the diffusion coefficient was set to be temperature-dependent.

The big difference between modeled salinity and observed one in figure 17 states clearly that it's unlikely to explain salinity distribution only by diffusion process. It must be another processes that influence salinity. One explanation can be the presence of an advective groundwater flow that has flushed the salinity away in this part of Netherlands. Another factor might be the presence of some confining layers. These layers have slowed down the salt

molecules movement decreasing thus the concentration gradient. Therefore, they have reduced the diffusion salinity rate.

de Vries (2007) in his chapter about groundwater in the Netherlands has stated that in the Roer Valley Graben, the Plio-Pleistocene sediment deposits are underlined by more than 1500 meters of fine grained sand and clay of marine origin from Miocene and late Oligocene ages. These low permeable basalt sediments (de Vries, 2007) might be the confining layer that has reduced the diffusion rate. However the NE-SW running fractures breaks this probability of confining layer. These fractures could be preferential path for vertical flow flushing away the salinity (supporting theory was made by de Vries (2007)). This is more plausible explanation because in one hand there is low concentration in the RVG, and near to it, on the German borders and within the same Breda formations, the fresh-salt water interface is about 1000meter (de Vries, 2007).Therefore it's more likely that the RVG marine sediment have been desalinated by fresh groundwater inflow from the past via these fractures.

b. Multiple synthetic wells diffusion

i. Results

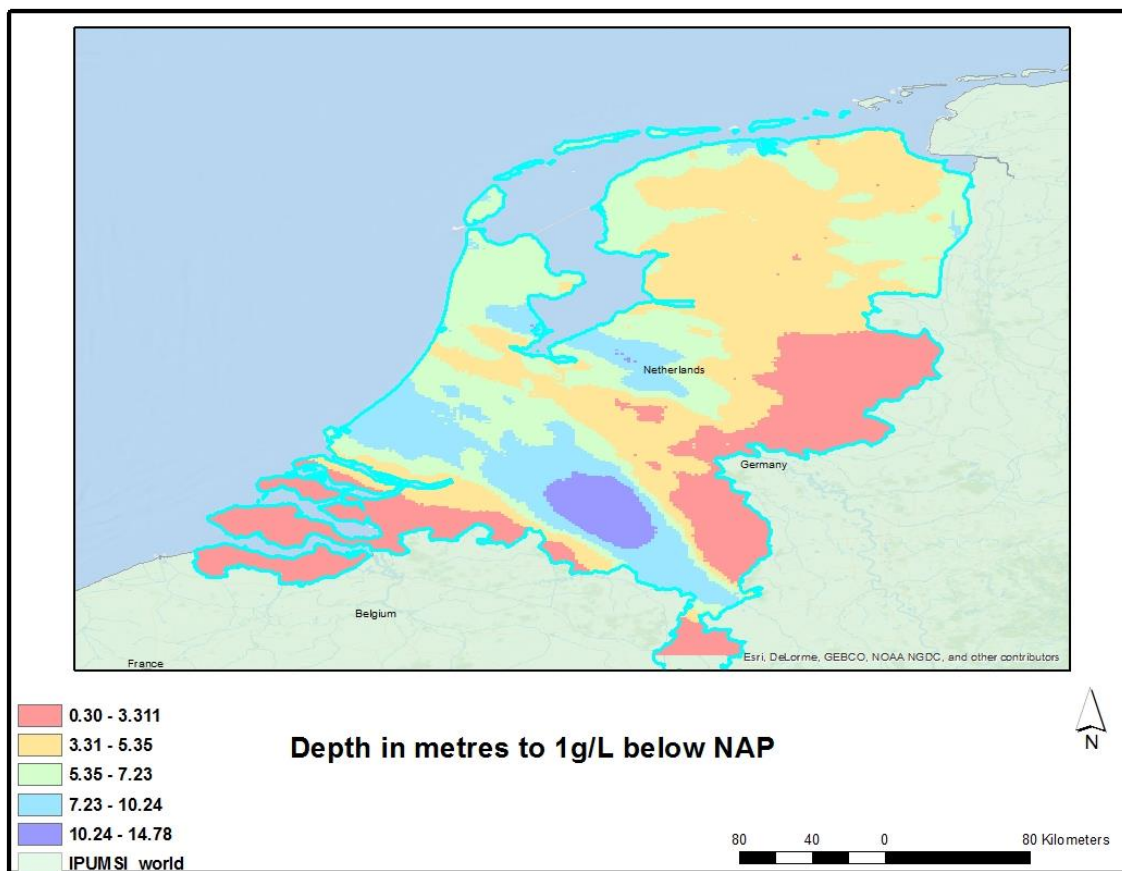


Figure 18: Modeled Fresh-saline water interface (1g/l) using diffusion model for multiple synthetic wells

The figure 18 represents the predicted fresh-saline water interface (1g/L) for multiple synthetic wells (diffusion only) using diffusion equation 7 with temperature dependent diffusion coefficient. The diffusion model has run throughout the 10573 synthetic wells with a model grid size of **100 m** and time step of 100000 **years** producing diffusion results of 2 * 2km spatial resolution. The fresh-saline water interface ranges from near surface 0.3 m in south west and south east (pink color) to approximately 15m south (purple color). The depth is function of burial depth rate, thickness of geological layers, and salinity of boundary condition (origin and surface salinity).

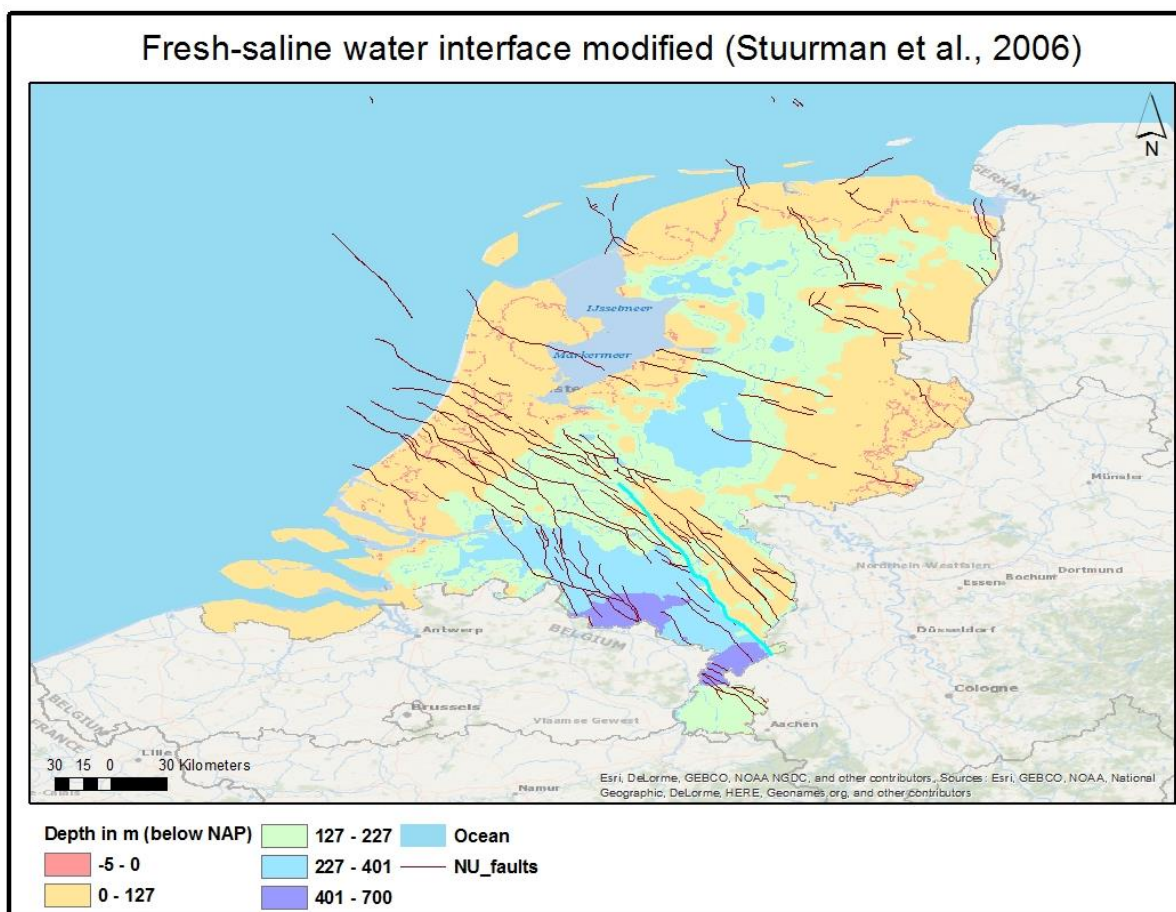


Figure 19: Fresh-Saline water interface (1g/L) modified
Source: (Stuurman et al., 2006) published by TNO

The figure 19 represents the measured depth to fresh-saline interface in Netherlands, based on a dense geo-electric surveys and well data (Stuurman et al., 2006). It ranges from 5 meter above sea level on the coast (east part) to 700 meters below sea level in the south and mostly a typical depth of maximum 127 meter below NAP.

The comparison between figure 18 and 19 (modeled salinity interface and observed salinity interface) shows that all over Netherlands, the observed fresh-saline water interfaces is much higher than the measured fresh water interface

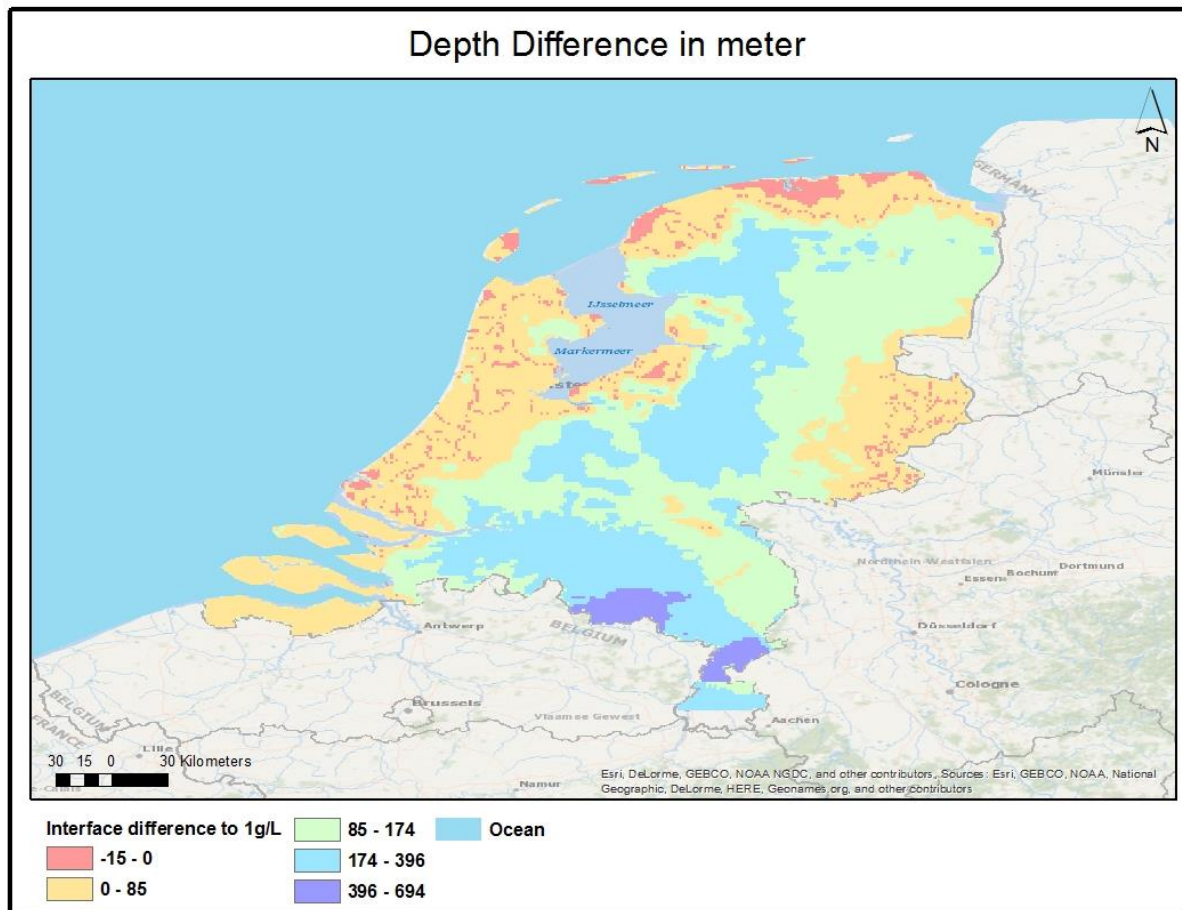


Figure 20: Difference between observed Fresh-saline water interface originated from (Stuurman et al., 2006) and diffusion only modeled fresh-saline interface (1g/L)

The figure 20 shows the depth difference to fresh-saline interface using two input raster. First one is the modeled fresh-saline interface for multiple synthetic wells (figure 18) and the other one observed fresh-saline water interface (figure 19). Figure 20 was obtained via a cell raster difference of figure 19 and figure 18.

The figure 20 is quite similar to figure 19 because there is more than 30 times difference magnitude between observed map and modelled map.

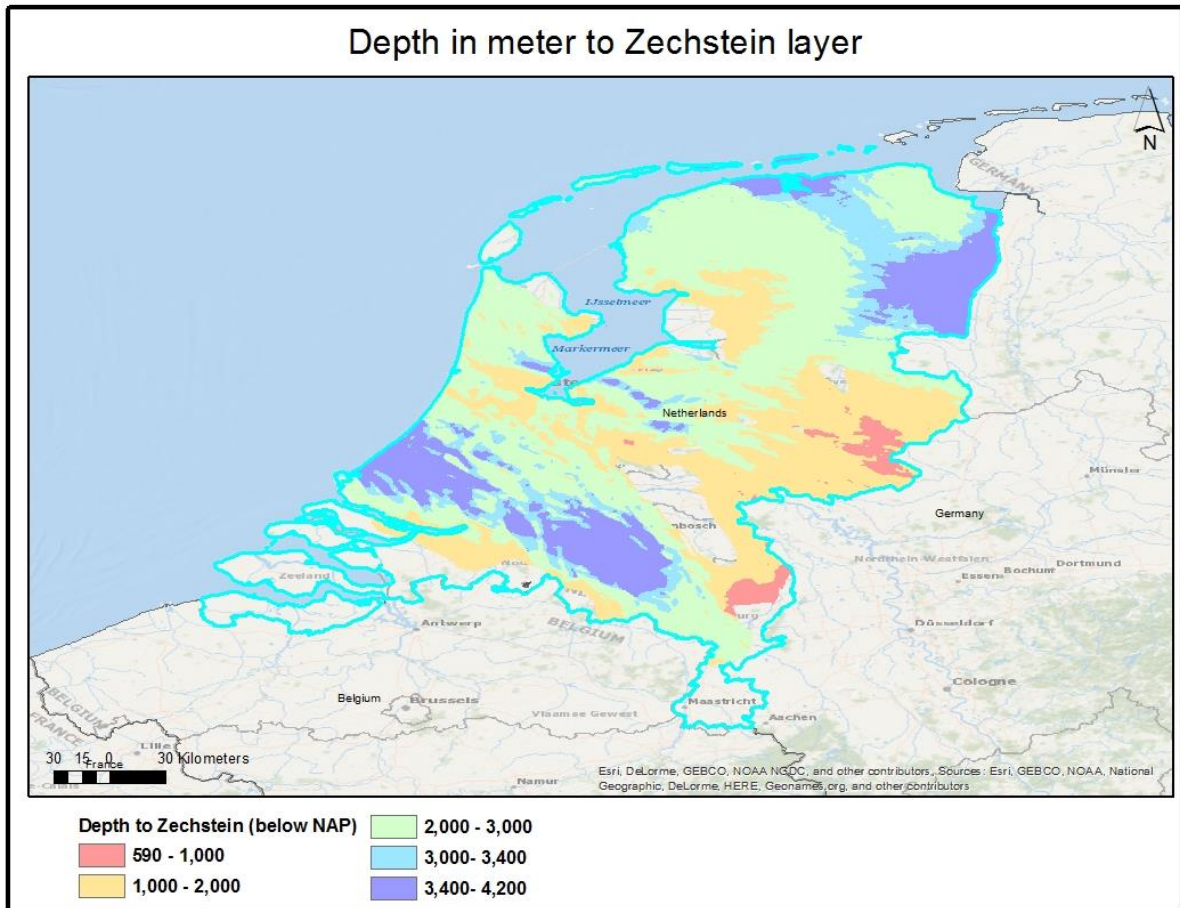


Figure 21: Depth in meter below NAP to the Zechstein modified

Source: (van Adrichem Boogaert and Kouwe, 1993)

The figure 21 shows the distance in meters to Zechstein layer below NAP based on a dense 2D and 3D seismic survey and well data. The depth repartition is between very deep (4000 meter) in north east-south west to medium depth in remaining part of the Netherlands (from 1000 until 3000 meter)

ii. Discussion

The modelled fresh-saline water interface distribution (figure 18) is due mainly:

- Distance to Pleistocene/Holocene deposits:

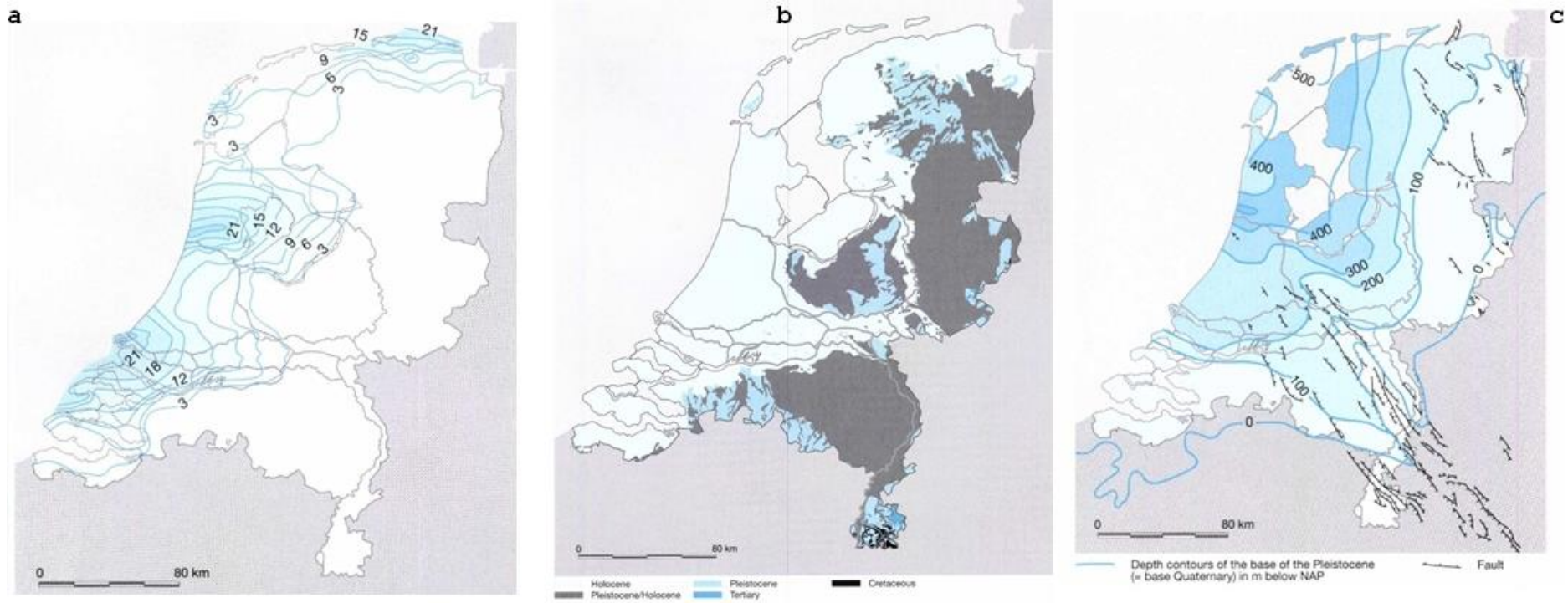


*Figure 22: a-Distance to base of the Holocene (below NAP); b-surface geology of Netherlands; c-distance to base of Pleistocene (Below NAP).
Source: (Dufour, 1998)*

In figure 18, the pink regions representing the modeled fresh-saline water interface is located at maximum 3.5 meter depth. The figure 22-c shows that in these regions, the depth to the Pleistocene which is the base of the quaternary is small (less than tens of meter). And during the interglacial periods of the Pleistocene, the sea advanced southeastwards (Dufour, 1998) so marine sediments laid in the south and east. These areas has also Holocene deposits (figure 22-b), in addition to some tertiary deposits that are 100% marine sediments.

A cross section (figure 23) was made from west to east displays how the base of the Pleistocene is getting shallower as we go to the east, therefore the distance to the salt water is small.

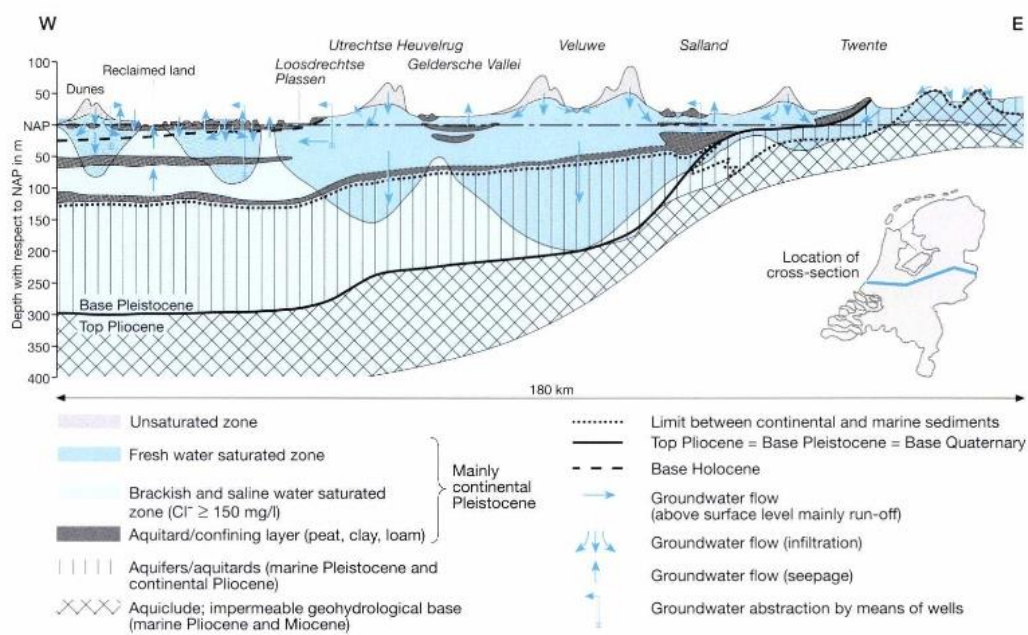


Figure 23: Hydrogeological cross section

Source : van de Ven et al,1986

In the orange to light green regions, the distance to the salt-fresh water is between 3.5 meters and 9.9 meters (second deepest). If the depth of the interface is related to the base depth of Pleistocene/ Holocene and existence of tertiary sediments (figure 22-b), which has a high depth (hundreds of meters), then a correlation can be made. Although this correlation exists but defining the exact ratio is hard because it is a big scale model.

The last zone with the dark blue color has the highest depth to the saline-fresh water interface. Although the figure 22-b shows the existence of Holocene/Paleocene and tertiary sediments in this region which are not very deep, the distance to the salt-fresh water interface is the deepest.

It might be that in addition to marine deposits, the diffusion in this part is influenced more by the distance to the evaporites source: Zechstein group.

- Distance to Zechstein (subsurface dissolution of evaporites)

There are 4 major big zones in dark blue where the distance to the Zechstein is the deepest. Two are located in the south and two in the north. For the one in the south east (in north Brabant province, 4600 meter deep), the correlated zone in the diffusion map represents the deepest fresh-saline water interface. This provide the explanation of this deepest salinity interface present in figure 18 (purple color). The other 3 red zones have the second highest distance to this interface, between 7 and 10 meters, and the matching location in Zechstein depth are proportional.

The distance to the Zechstein provides a typically matching behavior to the fresh-saltwater interface. Thus depth to solute source and diffusion distance principle is respected.

The high depth difference in fresh-saline water interface (figure 19) implies that the salinity distribution can not only be explained by diffusion. As it has been explained in single well diffusion model, it could also be the influence of groundwater flow.

- Groundwater flow

The fresh saline water interface is shallow in the coastal regions (figure 20). The surface elevation is low: 0 to 30 meter above mean sea level (figure 24). Pumping over these regions may have decreased the water table, which could have caused sea water intrusion and higher ground water salinity. Here it's more the local groundwater flow pattern and geology of first hundred meters -presence of clay and peat confining layers- (de Vries, 2007) that affects the distance to the salinity-fresh water interface..

From the combination of the figure 20 above and the surface elevation, it can be concluded that the highest places -for example the ice pushed ridges in the central part of the of the country (red zone) have a relatively deep fresh-saline interface compared to surrounding area. This may be due to the higher topography and relatively high permeability that drive groundwater flow and also to the displacement of saline water by meteoric water. This feature is more striking in the measured fresh-saline water interface map of Stuurman et al. (2006), showing again the influence of permeability and topography driven flow.

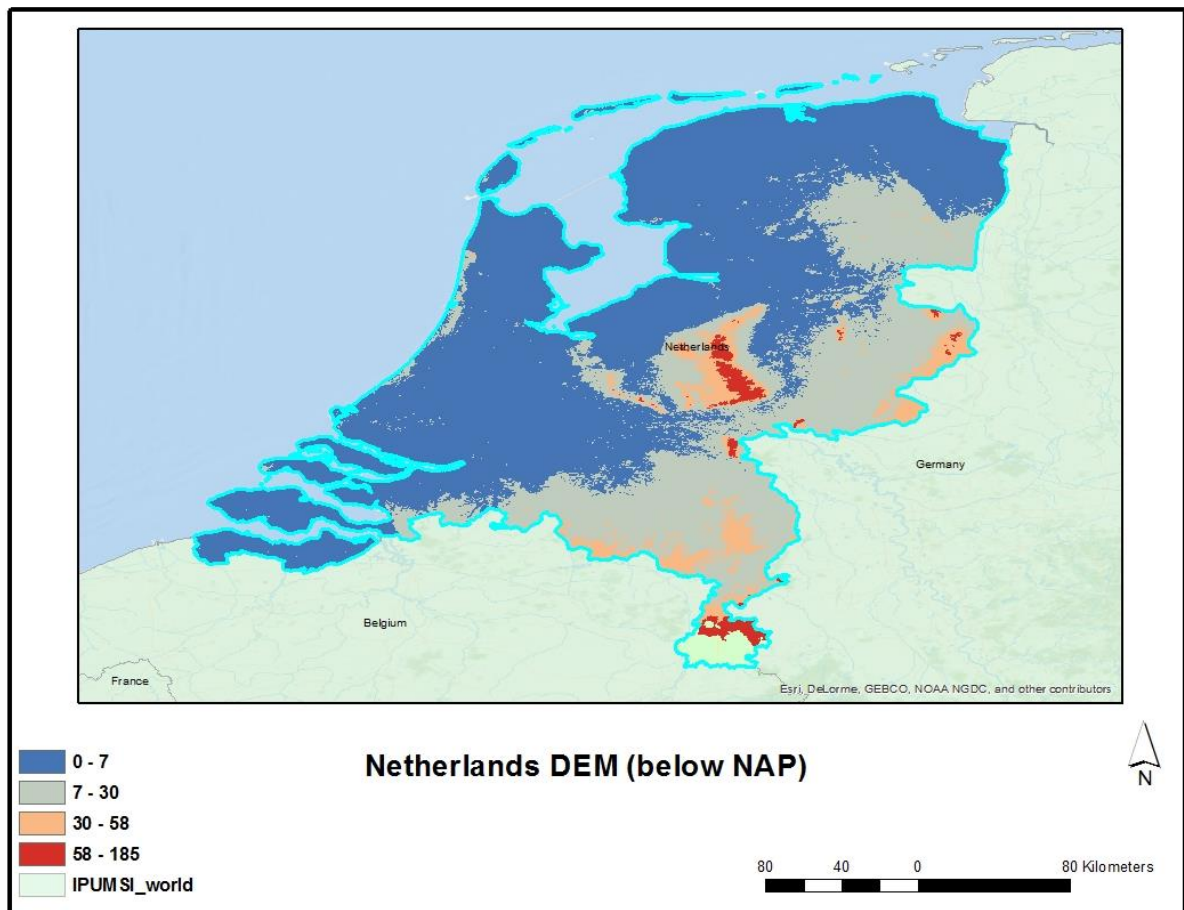


Figure 24: Digital elevation model modified

Source: Danielson, J. J., and D. B. Gesch (2011), *Global multi-resolution terrain elevation data 2010 (GMTED2010)*, US Geol. Surv. Open File Rep, 1073, 25

In the center of the Netherlands, there is no homogeneous trends but the observed fresh-saline interface is at medium depth (85 m to 300 m) in figure 19. There is no synchronized correlation between the observed and modelled interface-salinity map. This difference is due, in addition to difference in permeability, to different ground flow pattern present, sometimes local, sometimes intermediate and sometimes regional (Dufour, 1998).

In the east of Netherlands, the difference in fresh-saline water is at medium depth in figure 20. The groundwater flow influence the depth magnitude between observed salinity map and modelled salinity map.

Conclusion

The present research has shown how important could be the diffusion process and the influence of topography groundwater flow on salinity distribution. For that a solute diffusion model was set up and applied on well AST-02 and many other synthetic wells all over Netherlands. The output of the model pinpoints several key facts:

- Even the diffusion process is small but have a strong effect whenever on long timescales. The diffusion model output, has shown that fresh-saline water interface could be very shallow while taking only diffusion in consideration (figure 18).
- Marine deposits in Pleistocene and Holocene geological times affect the first hundred meters of salinity distribution.
- The distance to the evaporites (Zechstein) influences the depth to the fresh-saline water interface. The deepest is the Zechstein, the deepest is the interface (figure 21).
- The salinity mapping can not only be explained by the diffusion process. Indeed there is a magnitude difference between the modelled salinity and the observed one provided by Stuurman et al. (2006). This difference is due to the existence of groundwater flow pattern. This flow either local or regional is dominating the solute transport.

This work affinity is tracing groundwater throughout geological times using a diffusion salinity model. So on one hand, it could be interesting to set up a solute transport model and compare its output with Stuurman et al. (2006) map of Netherlands to have an idea about the extent of this influence. On the other hand, using the salinity from resistivity method will provide a powerful dataset of salinity all over the world.

References

- Batzle, M., Wang, Z., 1992. Seismic properties of pore fluids. *Geophysics* 57, 1396 – 1408.
doi:10.1190/1.1443207
- Courant, R., Friedrichs, K., Lewy, H., 1928. Uber die partiellen Differenzengleichungen der mathematischen Physik. *Math. Ann.* 100, 32–74. doi:10.1007/BF01448839
- Crain, E.R., 2006. *Crain's Petrophysical Handbook*, Crain's Petrophysical Handbook.
- de Jager, J., 2007. Geological development. *Geol. Netherlands* 5–26.
- de Vries, J., 2007. Groundwater, in: *Geology of the Netherlands*. pp. 295–315.
- Doornenbal, H., Stevenson, A., 2010. *Petroleum Geological Atlas of the Southern Permian Basin Area*. EAGE Publications bv.
- Dufour, F.C., 1998. *Groundwater in the Netherlands : facts and figures*. TNO, Delft.
doi:10.1017/CBO9781107415324.004
- DUNHAM, LANNY, Consulting Petrophys, 2001. Resistivity Logs Revisited. *Am. Assoc. Pet. Geol. Bull.* 85. doi:10.1306/8626CD75-173B-11D7-8645000102C1865D
- Hanor, J.S., 1994. Origin of saline fluids in sedimentary basins. *Geol. Soc. London, Spec. Publ.* 78, 151–174. doi:10.1144/GSL.SP.1994.078.01.13
- Heederik, J.P., Huurdeman, A.J.M., Vasak, L., 1988. *Geothermische Reserves Centrale Slenk, Nederland*. Explor. en Eval. Exploratie.
- Ingebritsen, S.E., Sanford, W.E., Neuzil, C.E., 2006. *Groundwater in Geologic Processes*. Cambridge University Press.
- Kuo, J., 1999. *Practical Design Calculations for Groundwater and Soil Remediation*.
- Luijendijk, E., Van Balen, R.T., Ter Voorde, M., Andriessen, P.A.M., 2011. Reconstructing the Late Cretaceous inversion of the Roer Valley Graben (southern Netherlands) using a new model that integrates burial and provenance history with fission track thermochronology. *J. Geophys. Res. Solid Earth* 116. doi:10.1029/2010JB008071
- NL Oil and Gas Portal, 2015a. DGM-deep v4.0 - onshore [WWW Document]. URL http://www.nlog.nl/en/pubs/maps/geologic_maps/DGM_deep_onshore.html (accessed 11.23.15).

- NL Oil and Gas Portal, 2015b. Logs, reports, measurements and geochemical analysis [WWW Document]. URL <http://www.nlog.nl/nlog/requestData/nlogp/allBor/queryForm?menu=act>
- Noel, C., 1990. The Origins of Kriging. *Math. Geol.* 22, 47–55.
- Sanchez, F., Garrabrants, A.C., Kosson, D.S., 2003. Effects of intermittent wetting on concentration profiles and release from a cement-based waste matrix. *Environ. Eng. Sci.* 20. doi:10.1089/109287503763336575
- Simpson, J.H., Carr, H.Y., 1958. Diffusion and nuclear spin relaxation in water. *Phys. Rev.* 111, 1201–1202. doi:10.1103/PhysRev.111.1201
- Stuurman, R., Essink, G.O., Broers, H.P., van der Grift, B., 2006. Monitoring zoutwaterintrusie naar aanleiding van de Kaderrichtlijn Water “verziltting door zoutwaterintrusie en chloridevervuiling.” TNO Bouw en Ondergr. Rapp. 84.
- van Adrichem Boogaert, H., Kouwe, W.F.P., 1993. Stratigraphic Nomenclature of the Netherlands, Revision and Update by RGD and NOGEPa. Geological Survey of The Netherlands.
- Vernier Software, 2016. Chloride and Salinity [WWW Document]. URL http://www2.vernier.com/sample_labs/WQV-15-COMP-chloride_salinity.pdf (accessed 4.8.16).
- Zagwijn, W.H., 1989. The Netherlands . during the Tertiary and the Quaternary: A case history of Coastal Lowland evolution. *Geol. en Mijnb.* 68, 107–120.
- Zhang, Y., Krause, M., Mutti, M., 2013. The Formation and Structure Evolution of Zechstein (Upper Permian) Salt in Northeast German Basin : A Review. *Open J. Geol.* 2, 411–426.

Appendix

Cation	$D_a(10^{-10} \text{ m}^2/\text{s})$	Anion	$D_w(10^{-10} \text{ m}^2/\text{s})$
H ⁺	93.1	OH ⁻	52.7
Na ⁺	13.3	F ⁻	14.6
K ⁺	19.6	Cl ⁻	20.3
Rb ⁺	20.6	Br ⁻	20.1
Cs ⁺	20.7	I ⁻	20.0
Li ⁺	10.3	HS ⁻	17.3
		HCO ₃ ⁻	11.8
Mg ²⁺	7.05	HCO ₄ ⁻	13.3
Ca ²⁺	7.93	NO ₂ ⁻	19.1
Sr ²⁺	7.94	NO ₃ ⁻	19.0
Ba ²⁺	8.48	H ₃ PO ₄ ⁻	8.46
Ra ²⁺	8.89		
Mn ²⁺	6.88	CO ₃ ²⁻	9.55
Fe ²⁺	7.17	SO ₄ ²⁻	10.7
Cr ³⁺	5.94	HPO ₄ ²⁻	7.34
Fe ³⁺	6.07	CrO ₄ ²⁻	11.2

Figure 25: Diffusion coefficient in water for some ions at 25 °C
Source: Li and Gregory (1974)

```

1 import arcpy
2 import timeit
3
4 start = timeit.default_timer()
5 k=0
6 shapefile = "well_bs.shp"
7 field_precision = 6
8 field_scale = 2
9 row_values = []
10 #arcpy.env.workspace = "C:/Users/simohamed/Desktop/travail/AT_depth_dec_2014_asc"
11 arcpy.env.workspace = "F:/HEG/master_thesis/extent_Roer_Valley_Graben/geoprocessing/"
12 field_name = ["Thick_NU", "Thick_NML", "Thick_CK", "Thick_KN", "Thick_SL", "Thick_AT", "Thick_RNRB", "Top_NU", "Bottom_NU", "Top_NML",
13 "Bottom_NML", "Top_CK", "Bottom_CK", "Top_KN", "Bottom_KN", "Top_SL", "Bottom_SL", "Top_AT", "Bottom_AT", "Top_RNRB", "Bottom_RNRB"]
14 raster=(arcpy.Raster("nu_thickness1"), arcpy.Raster("NMLM_thickness_dec_2014.asc"), arcpy.Raster("CK_thickness_dec_2014.asc"), arcpy.Raster("KN_thickness_dec_2014.asc"),
15 arcpy.Raster("S_thickness_dec_2014.asc"), arcpy.Raster("AT_thickness_dec_2014.asc"), arcpy.Raster("RNRB_thickness_dec_2014.asc"))
16 raster1= arcpy.Raster("NMLM_thickness_dec_2014.asc")
17
18 # add required field to our feature class
19
20 arcpy.AddField_management(shapefile, "Name", "TEXT")
21 for name in field_name:
22     arcpy.AddField_management(shapefile, name, "DOUBLE", field_precision, field_scale)
23 # using GetRasterProperties_management module, but it is very time consuming
24
25 xmin = arcpy.GetRasterProperties_management(raster1, "LEFT")
26 xmax = arcpy.GetRasterProperties_management(raster1, "RIGHT")
27 ymin = arcpy.GetRasterProperties_management(raster1, "BOTTOM")
28 ymax = arcpy.GetRasterProperties_management(raster1, "TOP")
29 cellSize = arcpy.GetRasterProperties_management(raster1, "CELLSIZE")
30 col_nbre = arcpy.GetRasterProperties_management(raster1, "COLUMNCOUNT")
31 row_nbre = arcpy.GetRasterProperties_management(raster1, "ROWCOUNT")
32
33 # convert to integer
34

```

Figure 26: Preview of Arcpy script for creating synthetic wells used in salinity diffusion model applied to Netherlands

Used Group in AST-02	Stratigraphical unit	Depth Top	Depth bottom
	QUATER. UNDIFF.	0	131
	Kieseloolite Formation	131	372
	upper Breda member	372	765
	Heksenberg Member	765	803
	lower Breda member	803	902
	Someren member	902	942
	Veldhoven Clay Member	942	1061
	Voort Member	1061	1275
	Steensel Member	1275	1297
	Rupel Clay Member	1297	1373
	Vessem Member	1373	1397
	Landen Clay Member	1397	1458
	Gelinden Member	1458	1483
	Heers Member	1483	1526
	Swalmen Member	1526	1531
	Houthem Formation	1531	1583
	Ommelanden Formation	1583	1603
	Aalburg Formation	1603	1608
	Sleen Formation	1608	1631
	Upper Keuper Claystone Member	1631	1648
	Dolomitic Keuper Member	1648	1651
	Middle Keuper Claystone Member	1651	1656
	Upper Muschelkalk Member	1656	1706
	Middle Muschelkalk Marl Member	1706	1747
	Muschelkalk Evaporite Member	1747	1767
	Lower Muschelkalk Member	1767	1870
	Upper Röt Fringe Claystone Member	1870	1917
	Röt Fringe Sandstone Member	1917	1963
	Lower Röt Fringe Claystone Member	1963	2016
	Solling Claystone Member	2016	2030
	Basal Solling Sandstone Member	2030	2035
	Hardeggen Formation	2035	2092
	Upper Detfurth Sandstone Member	2092	2111
	Lower Detfurth Sandstone Member	2111	2120
	Upper Volpriehausen Sandstone Member	2120	2215

	Lower Volpriehausen Sandstone Member	2215	2237
	Rogenstein Member	2237	2280
	Nederweert Sandstone Member	2280	2572
Zechstein	Zechstein Upper Claystone Formation	2572	2583
	Z3 Carbonate Member	2583	2592
	Grey Salt Clay Member	2592	2594
	Z2 Middle Claystone Member	2594	2625
	Z1 Middle Claystone Member	2625	2634
	Slochteren Formation	2634	2638
	Maurits Formation	2638	2942

Table 6: The stratification of Well NDW-01

Depth_AH	ILD	Measured Salinity ppm	salinity log scale
630	2.203075	2348.58	3.370805358
711	1.901207	1264.62	3.101960046
795	1.448872	1083.96	3.035013256
800	1.581356	1625.94	3.211104515
805	1.370977	1264.62	3.101960046
810	1.358408	903.3	2.95583201
817	1.422426	1264.62	3.101960046
824	1.333614	1445.28	3.159951993
880	1.279469	1083.96	3.035013256
904	1.256117	11020.26	4.042191841
905	1.183123	9033	3.95583201
980	1.339769	1445.28	3.159951993
997	2.99929	2529.24	3.402990042
1425	1.733921	25807.281	4.411742251
1429	2.748075	9755.64	3.989255766
1430	1.758043	24660.09	4.391994657
1435	1.678919	17135.601	4.233899341
1440	1.588655	20423.613	4.310132573
1445	1.588655	19926.798	4.299437518
1450	1.618191	53294.7	4.726684022
1465	1.815639	9033	3.95583201
1470	2.275251	7768.38	3.890330461
1470	2.275251	26015.04	4.415224498
1475	1.981663	15211.572	4.182174097

1480	1.875122	10198.257	4.008525952
1482	1.909983	22076.652	4.343933212
1484	1.766157	33060.78	4.519313096
1492	1.807297	39203.22	4.59332174
1510	1.832439	37938.6	4.579081301
1514	1.857931	46068.3	4.663402186
1521	2.143034	44442.36	4.647797113
1522	2.113634	62689.02	4.797191481
1532	1.972557	47874.9	4.68010788
1540	1.9188	76238.52	4.882174457
1545	1.9188	61063.08	4.785778706

Table 7 : Comparaison between ILD log and the measured salinity (log scale)

Used group in AST-02	Stratigraphical unit	Depth Top	Depth Bottom
	QUATER. UNDIFF.	0	195
	Kieseloolite Formation	195	360
	upper Breda member	360	718
	Heksenberg Member	718	800
	lower Breda member	800	867
	Someren member	867	952
	Veldhoven Clay Member	952	1088
	Voort Member	1088	1300
	Steensel Member	1300	1317
	Rupel Clay Member	1317	1391
	Vessem Member	1391	1410
	Reusel Member	1410	1458
	Landen Clay Member	1458	1488
	Gelinden Member	1488	1509
	Heers Member	1509	1538
	Swalmen Member	1538	1541
	Houthem Formation	1541	1582
	Ommelanden Formation	1582	1590
	Aalburg Formation	1590	2002
	Sleen Formation	2002	2019
Upper Germanic Trias Group RN	Dolomitic Keuper Member	2019	2030
	Red Keuper Claystone Member	2030	2034
	Lower Keuper Claystone Member	2034	2062
	Upper Muschelkalk Member	2062	2098
	Middle Muschelkalk Marl Member	2098	2108
	Muschelkalk Evaporite Member	2108	2115
	Lower Muschelkalk Member	2115	2153
	Upper Röt Fringe Claystone Member	2153	2178
	Röt Fringe Sandstone Member	2178	2243
	Lower Röt Fringe Claystone Member	2243	2322
	Solling Claystone Member	2322	2331
	Basal Solling Sandstone Member	2331	2337
	Lower Germanic Trias Group RB	Hardegsen Formation	2337
Upper Detfurth Sandstone Member		2388	2408
Lower Detfurth Sandstone Member		2408	2424
Upper Volpriehausen Sandstone Member		2424	2490
Lower Volpriehausen Sandstone Member		2490	2537
Rogenstein Member		2537	2656
Nederweert Sandstone Member		2656	2664

Table 8: The stratification of Well AST-01